Phosphodiesterase 2 Protects against Catecholamine-induced Arrhythmias and Preserves Contractile Function after Myocardial Infarction

Christiane Vettel, Marta Lindner, Matthias Dewenter, Kristina Lorenz, Constanze Schanbacher, Merle Riedel, Simon Lämmle, Simone Meinecke, Fleur Mason, Samuel Sossalla, et al.

Phosphodiesterase 2 Protects against Catecholamine-induced Arrhythmias and Preserves Contractile Function after Myocardial Infarction

Running title: *Vettel et al., PDE2 in arrhythmia and contractile function*

Christiane Vettel, PhD*; Marta Lindner*; Matthias Dewenter, MD*; Kristina Lorenz, PhD; Constanze Schanbacher; Merle Riedel, MD; Simon Lämmle, PhD; Simone Meinecke, MD; Fleur Mason, PhD; Samuel Sossalla, MD; Andreas Geerts; Michael Hoffmann; Frank Wunder, PhD; Fabian J. Brunner, MD; Thomas Wieland, PhD; Hind Mehel, PhD; Sarah Karam, PhD; Patrick Lechêne, BSc; Jérôme Leroy, PhD; Grégoire Vandecasteele, PhD; Michael Wagner, MD; Rodolphe Fischmeister, PhD[†,#]; Ali El-Armouche, MD[†,#]

From the Institute of Experimental and Clinical Pharmacology and Toxicology, University Medical Center Mannheim, Heidelberg University, Germany (C.V., T.W.); Department of Pharmacology, University Medical Center Göttingen (UMG) Heart Center, Georg August University Medical School Göttingen, Germany (C.V., M.D., M.R., S.M.); UMR-S 1180, INSERM, Université Paris-Sud, Université Paris-Saclay, Châtenay-Malabry, France (M.L., H.M., S.K., P.L., J.L., G.V., R.F.); Department of Molecular Cardiology and Epigenetics, University Hospital Heidelberg, Germany (M.D.); Institute of Pharmacology and Toxicology, University of Würzburg and Leibniz-Institut für Analytische Wissenschaften – ISAS – e.V., Dortmund, Germany (K.L., C.S.), Comprehensive Heart Failure Center, University of Würzburg, and West German Heart and Vascular Center Essen, Germany (K.L.); Institute of Pharmacology, University of Technology Dresden, Germany (S.L., M. W., A.EA.); Department of Cardiology and Pneumology, Center of Molecular Cardiology, UMG Heart Center, Georg August University Medical School Göttingen, Germany (F.M., S.S.); Department of Internal Medicine III: Cardiology and Angiology, University of Kiel, Germany (S.S.); BAYER Pharma AG, Wuppertal, Germany (A.G., M.H., F.W.); University Heart Center, Department of General and Interventional Cardiology, University Medical Center Hamburg-Eppendorf (F.J.B.). DZHK (German Centre for Cardiovascular Research), partner sites Heidelberg/Mannheim, Göttingen and Hamburg/Kiel/Lübeck, Germany (C.V., M.D., M.R., S.M., F.M., S.S., F.J.B., T.W.)

*[†]These authors contributed equally

[#]**Correspondence to**: Ali El-Armouche, Institute of Pharmacology, University of Technology Dresden, Medical Faculty Carl Gustav August, Fetscherstr. 74, 01307 Dresden, Germany. Phone: +49 351 458 6300, Fax: +49 351 458 6315; e-mail: ali.el-armouche@tu-dresden.de OR Rodolphe Fischmeister, INSERM UMR-S 1180, Université Paris-Sud, Faculté de Pharmacie, 5, Rue J.-B. Clément, F-92296 Châtenay-Malabry Cedex, France. Phone: 33.1.46.83.57.57; Fax 33.1.46.83.54.75; e-mail: rodolphe.fischmeister@inserm.fr

Word Count: 7746

Journal subject codes: Remodeling, Animal models of human disease, Arrhythmias-basic studies

Abstract

Rationale: Phosphodiesterase 2 (PDE2) is a dual substrate esterase, which has the unique property to be stimulated by cGMP, but primarily hydrolyses cAMP. Myocardial PDE2 is upregulated in human heart failure (HF), but its role in the heart is unknown.

Objective: To explore the role of PDE2 in cardiac function and heart disease.

Methods and Results: Pharmacological inhibition of PDE2 (BAY 60-7550, BAY) led to a significant positive chronotropic effect on top of maximal β-adrenoceptor (β-AR) activation in healthy mice. Under pathological conditions induced by chronic catecholamine infusions, BAY reversed both the attenuated β-AR mediated inotropy and chronotropy. Conversely, ECG telemetry in heart specific PDE2 transgenic mice (TG) showed a marked reduction in resting as well as in maximal heart rate, while cardiac output was completely preserved due to greater cardiac contraction. This well tolerated phenotype persisted in elderly TG with no indications of cardiac pathology or premature death. Molecular studies on the cardiomyocyte level showed lower β-AR stimulation of contractility, Ca^{2+} transients and L-Type Ca^{2+} current. During arrhythmia provocation induced by catecholamine injections, TG animals were resistant to triggered ventricular arrhythmias. Accordingly, Ca^{2+}-spark analysis in isolated TG cardiomyocytes revealed remarkably reduced Ca^{2+}-leakage and lower basal phosphorylation levels of Ca^{2+}-cycling proteins including ryanodine receptor type 2. Moreover, TG demonstrated attenuated ventricular dysfunction and a strong trend toward prolonged survival after myocardial infarction.

Conclusion: Endogenous PDE2 contributes to heart rate regulation. Greater PDE2 abundance protects against arrhythmias and improves contraction force after severe cardiac insult. Activating myocardial PDE2 may thus represent a novel intracellular anti-adrenergic therapeutic strategy protecting the heart from arrhythmia and contractile dysfunction.

Key words: phosphodiesterase, β-adrenoceptors, heart rate, arrhythmia

Nonstandard Abbreviations and Acronyms

AR	adrenoceptor
BAY	PDE2-inhibitor BAY 60-7550
BPs	systolic blood pressure
BPd	diastolic blood pressure
bpm	beats per minute
BW	body weight
cAMP	cyclic adenosine monophosphate
cGMP	cyclic guanosine monophosphate
CO	cardiac output
CSQ	calsequestrin
DOBU	dobutamine
FAS	fractional area shortening
HF	heart failure
HR	heart rate
$I_{Ca,L}$	L-type Ca^{2+} channel current
ISO	isoproterenol
IVA	ivabradine
LAD	left anterior descending coronary artery
LTCC	L-type Ca^{2+} channel
LVW	left ventricular weight
METO	metoprolol
MI	myocardial infarction
NCX	sodium-calcium exchanger
NO	nitric oxide
NP	natriuretic peptide
PDE	phosphodiesterase
PLB	phospholamban
RYR2	ryanodine receptor type 2
SCaW	spontaneous Ca^{2+} waves
SR	sarcoplasmic reticulum
TG	PDE2-transgenic
VT	ventricular tachycardia
WT	wildtype

Heart failure (HF) is among the most common causes of morbidity and mortality worldwide. A characteristic feature of this pathophysiological condition is a chronic activation of the sympathetic nervous system[1]. Although initially aimed to maintain cardiac output, constant stimulation of β-adrenoceptors (β-ARs) results in molecular and structural changes, such as hypertrophy, cardiac fibrosis, and electromechanical dysfunction. This process creates a setting for lethal cardiac arrhythmias, which may account for approximate 40% of deaths in patients with HF[2, 3]. Moreover, increased resting heart rate and lower heart rate variability are significant prognostic risk factors for mortality and cardiovascular outcome[4, 5]. The sympathetically stressed heart responds with desensitization mechanisms which involve the reduction of functional β_1-AR and the redistribution β_2-AR at the plasma membrane[6, 7], but also a modulation in abundance and/or activity of intracellular key effectors, downstream of receptor activation[8, 9]. Even though β-AR desensitization may further compromise contractile performance, it nevertheless appears to be a protective adaptation against catecholamine toxicity[10]. Accordingly, pharmacological blockade of receptor activation by β-blockers to date is a central strategy in attenuating HF progression[11]. In this context, the extent of heart rate reduction by β-blockers appears to be of particular importance for the clinical outcome in HF[12]. However, not all patients receive or tolerate the necessary dose to substantially improve prognosis[13].

In contrast to β-AR signaling, which is mainly mediated by the second messenger cyclic adenosine monophosphate [14], the actions of cyclic guanosine monophosphate (cGMP) generated by either natriuretic peptides (NP) or nitric oxide (NO) are considered to be beneficial in HF partially because they may oppose cAMP-induced stress remodeling[15-18]. Both cAMP and cGMP are regulated in level and subcellular distribution by cyclic nucleotide hydrolyzing phosphodiesterases (PDEs). Their degradation is a highly compartmentalized process, allowing the distinction of different extracellular stimuli to maintain the specificity of downstream target activation[19]. Among the PDE families expressed in the heart, PDE2 has the unique property to be activated by cGMP via binding of the nucleotide to a regulatory GAF-B domain located at its N-terminus[20, 21]. The conformational change induced by this allosteric mechanism increases cAMP hydrolysis 10- to 30-fold thus staging PDE2 in the center of a negative cGMP/cAMP crosstalk[22]. Evidence for such a crosstalk regarding the cardiovascular system includes the cGMP-mediated decrease in ventricular and atrial L-type Ca^{2+} channel current ($I_{Ca,L}$) in various species including man[23, 24], β_3-AR-dependent regulation of protein kinase A in cardiomyocytes[25], and the ANP-mediated reduction in aldosterone production in adrenal glomerulosa cells[26]. Unlike the described downregulation of cAMP-degrading PDE3 and some isoforms of PDE4[27, 28], myocardial PDE2 is upregulated in human HF. We showed that the upregulation of ventricular PDE2 is a direct consequence of chronic β-AR overstimulation and part of the β-AR desensitization machinery[29]. However, the consequences of higher abundance and activity of PDE2 on cardiac function are largely unknown.

In the present study, we show that in healthy hearts, PDE2 tonically reduces heart rate, but controls both β-AR chronotropic and inotropic responsiveness under stressed conditions *in vivo*. Moreover, we generated a cardiac PDE2-transgenic (TG) mouse line to evaluate short and long term effects of chronically increased PDE2 activity in the heart. Our study reveals that greater PDE2 abundance lowers heart rate without impairment of cardiac contractility *in vivo* and protects against ventricular arrhythmias by preventing Ca^{2+}-leakage from the sarcoplasmic reticulum (SR). In experimental myocardial infarction, higher PDE2 abundance improved ventricular function and may even prolong survival.

Methods

For a detailed description of methods including surgical procedures see Online Supplement Material.

Chronic isoproterenol administration: Isoproterenol (ISO, 30 µg/g/d, Sigma-Aldrich) was delivered to mice by subcutaneously implanted osmotic minipumps (Alzet, model 2002).

Application of dobutamine, BAY 60-7550 and metoprolol for echocardiographic experiments: Anesthetized mice were analyzed by echocardiography first under basal conditions and then 5 min after the injection of dobutamine (DOBU, i.p., 10 mg/kg). When indicated, BAY (i.p., 3 mg/kg) was applied 10 min post DOBU injection, and after an additional period of 10 min cardiac function was again echocardiographically monitored. For metoprolol studies, doses from 1 to 100 mg/kg (i.p.) were cumulatively applied with 10 min intervals between injections and echocardiographic measurements.

Generation of PDE2 transgenic mice: PDE2-TG mice were generated by using a plasmid containing the murine sequence of the splice variant PDE2A3 (NM_001008548.3). Expression was set under the control of the human α-myosin heavy chain promoter to ensure cardiac specificity[30]. Transgenesis was achieved by pronucleus injection of linearized plasmids into isolated zygotes of a FVB/N donor strain. Successful transformation of the offspring was assessed by PCR and overexpression levels were determined by immunoblot analysis. Resulting founder lines were crossed into a C57Bl/6 background.

ECG-telemetry recordings and arrhythmia provocation: ECGs were recorded in freely moving unrestrained mice. Arrhythmia provocation was performed by double injections of isoproterenol (ISO, i.p. 2 mg/kg) separated by an interval of 30 min; analysis was performed for 90 min after the first injection.

Isolation of adult mouse ventricular myocytes: Adult mouse ventricular myocytes were isolated by Langendorff perfusion using a Ca^{2+}-free Tyrode's solution containing liberase as described previously[31].

cAMP measurements by FRET: Adult mouse ventricular myocytes mice were infected with an adenovirus encoding the Epac-S^{H187} cAMP FRET probe for 24 h[32]. Changes in cAMP levels were assessed by YFP/CFP emission ratios.

Patch-Clamp studies: L-type Ca^{2+} currents ($I_{Ca,L}$) were recorded in the whole-cell configuration of the patch-clamp technique[33].

Ca^{2+} spark analysis: Ca^{2+} spark measurements were performed on a laser scanning confocal microscope (LSM 5 Pascal, Zeiss). Fluorescence images of Fluo-3 AM (10 µmol/L, Molecular Probes) loaded ventricular myocytes were recorded in the line-scan mode.

Measurement of Ca^{2+} transients, sarcomere shortening, SR Ca^{2+} leak and load: Isolated mouse ventricular cardiomyocytes were loaded with 3 µmol/L Fura-2 AM (Invitrogen). Sarcomere shortening and Fura-2 ratio (measured at 512 nm upon excitation at 340 and 380 nm) were simultaneously recorded using spectrofluorimeter coupled with a video detection system (IonOptix) as previously described[33]. Myocytes were electrically stimulated at a frequency of 0.5 Hz.

Immunoblot analysis: Protein samples were prepared from pulverized ventricular myocardium and lyzed in a buffer containing 30 mmol/L Tris/HCl (pH 8.8), 5 mmol/L EDTA, 30 mmol/L NaF, 3% SDS, and 10% glycerol. Samples were separated in denaturizing acrylamide gels and subsequently transferred onto nitrocellulose or PVDF membranes. After blocking the membranes with Roti®-block (Carl Roth) for 1 h, the incubation with anti-calsequestrin (1:1,000, ThermoScientific), anti-SERCA2a, anti-PDE2 (each 1:200, Santa

Cruz), anti-pPLB-S16, anti-pPLB-T17, anti-PLB, anti-pRYR2-S2808, anti-pRYR2-S2814 (each 1:5,000, Badrilla), and anti-RYR2 (1:2,000, Sigma-Aldrich) was carried out over night at 4°C. After incubation with appropriate secondary antibodies for 1 h, proteins were visualized by enhanced chemoluminescence (VersaDoc, Biorad) and quantified with Quantity One software (Biorad).

Ligation of the anterior descending artery

At the age of 10-14 weeks, mice were subjected to permanent ligation of the left anterior descending coronary artery (LAD) to induce myocardial infarction. After anesthesia was induced using 10% ketamine/ 2% xylazine i.p., the chest was opened between the third and the fourth rib. A 8−0 silk suture was used to occlude the LAD. Animals received buprenorphine (0.05–0.1 mg/kg, s.c.) for post-operative analgesia. ECG-telemetry recordings were performed for 2 weeks after LAD ligation.

Statistics: Results are presented as mean±SEM. Data sets were compared by Student's *t*-test, one-way ANOVA followed by Newman Keuls multiple comparison test, two-way ANOVA, Fisher's exact test or Pearson correlation according to the experimental setting. P values of less than 0.05 were considered statistically significant.

Results

Consequences of pharmacological PDE2 inhibition on cardiac function in vivo

To characterize the contribution of PDE2 to cardiac function under chronic β-AR stimulation *in vivo*, we subjected mice to ISO infusions (30 mg/kg/d for 7d) or NaCl (0.9%) as control. As expected, ISO treated animals developed prominent cardiac hypertrophy, indicated by an increase in left ventricular weight to body weight ratio from 3.6±0.2 to 4.7±0.1 mg/g ($p<0.05$, Suppl. Fig. 1). After chronic ISO treatment, the positive chronotropic and ionotropic effects of DOBU were abrogated, indicating desensitization of the β-ARs (Fig. 1). This was completely reversed by inhibition of PDE2 with BAY (3 mg/kg), restoring β-AR responsiveness to the level observed in the control group (Fig. 1). Interestingly, PDE2 inhibition also had an effect on control mice, almost doubling the impact of β-AR stimulation on heart rate over the average basal heart rate of 424±18 bpm from 95±29 to 170±23 bpm (Fig. 1B). The dosage of 3 mg/kg was chosen according to recent publications regarding *in vivo* experiments in rodents[34] and unpublished pharmacokinetic studies provided by BAYER. This restriction of PDE2 to chronotropic regulation under physiological conditions was supported by a study on beagle dogs treated with increasing doses of BAY (3, 10, and 30 mg/kg). In line with the murine model, the inhibition of PDE2 predominantly resulted in acceleration of heart rate (10 mg/kg: +20%; 30 mg/kg: +28%, Suppl. Fig. 2A), while stroke volume (SV), cardiac output (CO) and systolic (BPs) as well as diastolic blood pressures (BPd) remained largely unchanged (Suppl. Fig. 2B). Taken together, the role of PDE2 seems restricted to heart rate regulation under physiological conditions, while its stress-induced upregulation contributes to the desensitization of both β-AR-induced increases in heart rate and contraction force.

Effect of PDE2 overexpression on heart rate and cardiac function

To gain insight into the consequences of higher cardiac PDE2 levels, we generated transgenic (TG) mouse lines which overexpress PDE2 about 6- to 15-fold specifically in cardiomyocytes (Fig. 2H; Suppl. Fig. 3, 4). The low expressing (6-fold) line TG-4808 did not show any overt phenotype (Suppl. Fig. 3). In contrast, the ~10-fold overexpressing line TG-4320 (Fig. 2H) analyzed at 2 months displayed a substantial lower basal and dobutamine (DOBU)-stimulated maximal heart rate compared to wildtype (WT) with an average difference of 77±17 and 98±14 bpm, respectively (Fig. 2B). Basal contraction force measured as fractional area shortening (FAS) was higher in TG-4320 than in WT (37±1% vs. 32±1%), while maximal DOBU-stimulated contractility remained unaffected (80±3% in WT and 77±2% in PDE2-TG, Fig. 2A). In line with this, the lower heart rate combined with higher basal contraction produced a cardiac output virtually identical to that of WT controls (Fig. 2C). The higher contraction force in TG-4320 was not associated with cardiac hypertrophy as left ventricular weight to body weight ratio or heart weight to tibia length did not differ between WT and PDE2-TG mice (Fig. 2G, 3C). PDE2-TG displayed preserved susceptibility to β-AR blockade by metoprolol regarding the decrease both in heart rate and FAS with IC_{50} values that paralleled WT controls (Fig. 2D-F, Suppl. Fig. 5). Interestingly, while maximal doses of metoprolol (100 mg/kg) reduced heart rate to a similar extent in WT and PDE2-TG (332±15 and 306±8 bpm, respectively), FAS of PDE2-TG was higher under β–AR blockade compared to WT controls (31±2% in WT *vs.* 44±2% in PDE2-TG, Fig. 2D, F). The specific phenotype of lower HR with preserved cardiac performance was confirmed in a second independent transgenic line (TG-4811) with even higher overexpression levels (15-fold, Suppl. Fig. 4) excluding possible insertion artefacts. In accordance with recently published guidelines for transgenic mice[35] the lower expressing TG-4320 was chosen for the following experiments and will hence be referred to as PDE2-TG or TG.

Next, we analyzed the effects of PDE2 abundance on cardiac morphology and performance throughout most of the animals' life span including elderly mice. Notably, during 18 months of serial echocardiography, low heart rate and higher cardiac performance were preserved with no indication of functional decline, maladaptive remodeling or premature death (Fig. 3). The prominent impact on basal heart rate prompted us to investigate the effect of PDE2 on heart

rate regulation by telemetric ECG recordings in unrestrained, freely moving mice. Circadian analysis over the course of 24 h confirmed significantly lower heart rates in PDE2-TG animals during low activity daytime (∆105±17 bpm) as well as high activity nighttime (∆90±24 bpm, Fig. 4A, B and Suppl. Fig. 6A, B). Accordingly, analysis of the respective RR intervals recorded for 24 h showed longer average intervals in PDE2-TG demonstrated by a rightward shift of the Gaussian distribution curve (Fig. 4C). The difference in RR pattern was further confirmed by Poincaré analysis (Suppl. Fig. 6C, D). Notably, the broadening of the RR distribution as well as the significantly higher standard deviation from average RR-intervals indicate higher heart rate variability in PDE2-TG compared to WT animals (Fig. 4D). Thus, overexpression of PDE2 recapitulates the classical shift in sympathetic/parasympathetic balance as observed during an increased parasympathetic control of heart rate regulation[36]. However, PDE2-TG displayed the same relation of heart rate and physical activity as WT littermates, indicating preserved chronotropic competence (Fig. 4E). Basal heart rate reduction with maintained autonomic control has been allocated to a decrease in hyperpolarization-activated cyclic nucleotide-gated (HCN) channels activity[37]. Therefore we investigated the impact of HCN-blocker ivabradine (IVA; i.p. 5 µg/g) on heart beat frequency (Fig. 4F, Suppl. Fig. 6E). WT and TG animals showed similar susceptibility to IVA treatment displaying no significant difference in either lowest heart rate (348±23 and 319±17 bpm, respectively) or average heart rate reduction (158±10 bpm for WT and 128±14 for TG).

Impact of PDE2 overexpression on cAMP levels and Ca^{2+} cycling

To study the cellular mechanisms involved in PDE2 action, we investigated how PDE2 overexpression affects intracellular cAMP levels ($[cAMP]_i$). For that, we assessed real time changes in β-AR-induced $[cAMP]_i$ by FRET measurements in isolated ventricular myocytes infected with an adenovirus expressing the FRET-based cAMP probe Epac-S^{H187} [32]. The response to a 15 s application of ISO (30 nmol/L) was markedly blunted in PDE2-TG myocytes which showed an average change over basal of 17% compared to an average of 120% displayed by WT animals (Fig. 5A).

Next, we analyzed the consequences of the reduced accumulation of $[cAMP]_i$ on cellular Ca^{2+} handling in PDE2-TG mice. In line with previous publications, PDE2 overexpression markedly attenuated the β-AR induced increase in $I_{Ca,L}$ from 35% in WT to 8% in PDE2-TG (Fig. 5B), while basal $I_{Ca,L}$ amplitude remained unaffected (data not shown). This effect was fully reversed by PDE2 inhibition with BAY (Fig. 5C). Accordingly, Ca^{2+} transient and contractility analysis in field stimulated isolated ventricular myocytes revealed an attenuation of the β-AR response to ISO, while basal contractility and Ca^{2+} transients were similar between WT and PDE2-TG mice (Suppl. Fig. 7). SR Ca^{2+} load and fractional release were evaluated during the SR leak protocol (see below) by rapid application of 10 mmol/L caffeine. As expected, SR Ca^{2+} load as well as the fraction of released Ca^{2+} from the SR during systole significantly increased in WT derived ventricular myocytes after β-AR stimulation. In contrast, the ISO-induced increase in fractional SR Ca^{2+} release was absent in PDE2-TG, while SR Ca^{2+} content was not affected neither under basal nor stimulated conditions (Fig. 5D, E). This observation is in line with the lower β-AR response of systolic Ca^{2+} amplitude and force development measured in myocytes from PDE2-TG (Suppl. Fig. 7).

Arrhythmia provocation

To test the effect of greater PDE2 abundance under acute β-AR stress, animals received two injections of ISO (2 mg/kg) separated by an interval of 30 min[38]. As expected from echocardiographic analysis (Fig. 2B) and heart rate/activity correlation (Fig. 4E), PDE2-TG displayed a lower maximal heart rate upon β-AR stimulation (693±9 bpm in WT *vs*. 610±5 bpm in PDE2-TG), while chronotropic adaptation, i.e. absolute increase over basal heart rate, was maintained (157±18 bpm and 154±11 bpm, respectively, Fig. 6A, B). ECG was monitored for arrhythmic events such as ventricular extra systoles (VES), salvos and ventricular tachycardia (VT) over a period of 90 min after the first injection. All animals tested developed VES with frequency of occurrence increasing starting approximately 15 min after

the second injection of ISO (Suppl. Fig. 8A). The total number of VES was significantly lower in PDE2-TG (73±12 in WT *vs.* 30±9 in PDE2-TG, Fig. 5C). Importantly, only 1 out of 7 TG animals displayed severe arrhythmic events in form of VTs, while VTs were common incidents in WT animals where 6 out of 7 animals were affected (Fig. 6D, E). This finding was further confirmed *in vitro* where isolated WT ventricular myocytes exposed to ISO showed frequent occurrences of spontaneous Ca^{2+} waves (sCaW) which were abrogated in myocytes isolated from PDE2-TG mice (Fig. 6F, G).

Ca^{2} leak and Ca^{2+} handling proteins

Since ISO-induced arrhythmias are to a large extent caused by an increased diastolic Ca^{2+} leak from the sarcoplasmic reticulum (SR) via the ryanodine receptor (RYR2)[39-41], analysis of Ca^{2+} sparks was conducted to estimate Ca^{2+} leakage. PDE2-TG animals revealed a trend to a lower number of sparks under basal conditions and a complete abrogation of the increase in spark frequency after application of ISO, indicating the likely underlying cause of the reduced arrhythmia burden of PDE2-TG mice after ISO injection (Fig. 7A, B). This was further confirmed by assessing the SR Ca^{2+} leak as the difference between the Fura-2 ratio with and without RYR2 blocker tetracaine (1 mmol/L), using a $0Na^{+}/0Ca^{2+}$ solution to prevent Ca^{2+} extrusion by the Na^{+}/Ca^{2+} exchanger (Suppl. Fig. 9).

To explore the molecular mechanisms of a reduced Ca^{2+} leak, we performed immunoblot analysis of key Ca^{2+} handling proteins (Fig. 7C-G). Consistent with the preserved SR Ca^{2+} load in PDE2-TG mice (Fig. 5D), we did not find differences between WT and PDE2-TG mice in regard to the expression of SERCA2a, PLB or RYR2. PLB phosphorylation was significantly reduced at S16 and milder also at T17. Most strikingly, we found a reduction of RYR2 receptor phosphorylation at the described Ca^{2+}/calmodulin-dependent kinase II (CaMKII) phosphorylation site, S2814, which has been linked to diastolic Ca^{2+} leakage, but not at the putative PKA site S2808.

Arrhythmia development and cardiac function after myocardial infarction

To induce myocardial infarction (MI), mice were subjected to ligation of the left anterior descending artery (LAD). While infarct size was similar in both groups (Fig. 8C), PDE2-TG were markedly protected against ventricular failure with an ejection fraction of 47±5% compared to 31±4% in WT (Fig. 8A, B) at 14d after MI. The overall VT incidence was only slightly and not significantly lower in PDE2 TG than in WT: 62.5% of the WT and 53.3% of PDE2-TG developed VTs in the first 40 h following MI (Fig. 8E). However, only 30% of WT with VTs survived the first 7d, whereas none of the PDE2-TG with VTs suffered from an early death (Fig. 8F). Moreover, all early WT deaths were preceded by VTs, while PDE2-TG did not show this correlation (Fig. 8G). Further analysis of WT and PDE2-TG VT quality suggested a tendency towards long VTs (>20s) in WT animals with early deaths (3 out of 7), which occurred neither in WT survivors nor in PDE2-TG (Suppl. Fig. 10, Fig. 8H). Overall, over 86% of PDE2-TG survived the early phase post MI, while only 56% of WT animals endured more than 7d (Fig. 8D, p=0.06). No further deaths occurred in either group between day 8 and day 14 (endpoint of intervention).

Discussion

Myocardial PDE2 is upregulated in human as well as in experimental HF but its physiological and pathological role in the heart remained unknown. Here, we show that heart rate regulation is the predominant physiological role of PDE2. Specific inhibition of PDE2 in dogs and mice led to an exclusive increase in heart rate, while overexpression of PDE2 resulted in its decrease. Under chronic β-AR activation, however, PDE2 contributes to myocardial β-AR desensitization, protecting the heart from excessive sympathetic stress. Moreover, under acute β-adrenergic stress, higher PDE2 abundance effectively protects against ventricular arrhythmia without compromising contractile performance *in vivo*. In the setting of MI, PDE2 TG showed improved ventricular function compared to WT.

Role of PDE2 in heart rate regulation

The modern concept of heartbeat initiation is based on the mutual interplay between ion channels of the cell membrane ("membrane clock") and cellular Ca^{2+} cycling ("Ca^{2+} clock")[42, 43]. The most prominent targets of sympathetic heart rate modulation are the funny current (I_f), mediated by cAMP-dependent regulation of HCN channels and PKA-dependent phosphorylation of L-type Ca^{2+} channels (LTCC) as well as of SR Ca^{2+} cycling proteins[44]. So far, PDE2 has been shown to contribute to myocardial Ca^{2+} cycling by modulating $I_{Ca,L}$ not only in ventricular, but also in atrial and sinoatrial nodal cells[23, 24, 45]. These findings are consistent with the attenuated β-AR responsiveness regarding $I_{Ca,L}$ and SR Ca^{2+} release observed in PDE2-TG derived ventricular myocytes. Moreover, the close interplay between $I_{Ca,L}$, RYR2-mediated Ca^{2+} release and SERCA/PLB-dependent filling of the SR suggests that PDE2 is involved in the regulation of the Ca^{2+} clock[43]. However, while in the ventricular myocardium *in vivo* contraction force was unaffected in PDE2-TG, PDE2-TG exhibited lower basal as well as maximal heart rates, but retained β-AR induced control of pacemaker activity. This particular chronotropic phenotype has remarkable parallels with a cardiac cAMP-binding deficient HCN4 mutation analyzed in mice and humans[46, 37]. Notably, while HCN-blockade with IVA had no effect in mice expressing the mutated channel[46], PDE2-TG mice were still sensitive to IVA treatment indicating a remaining contribution of I_f to basal heart rate regulation. This study shows for the first time, that PDE2 is a major player in heart rate regulation *in vivo*, most likely by affecting both membrane and Ca^{2+} clock.

Role of PDE2 in propensity to arrhythmia and in contractility

There is substantial evidence that generation of delayed afterdepolarizations due to increased diastolic Ca^{2+} leak from the SR via RYR2 and the subsequent depolarizing activity of the Na^+/Ca^{2+} exchanger (NCX) is the main underlying mechanism for triggered arrhythmias[47]. A central role in this dysfunction of Ca^{2+} cycling has been attributed to the phosphorylation of RYR2 at the CaMKII site S2814 and the associated facilitation of diastolic Ca^{2+}-release[40, 41, 48]. Our conclusion that PDE2-TG are less susceptible to arrhythmia provocation induced by acute β-AR stimulation due to a significantly lower Ca^{2+}-spark frequency as well as lower RYR2-S2814 phosphorylation fits well to this model. At the cardiomyocyte level, efficacy of β-AR-induced increase in sarcomere shortening was significantly attenuated, as were efficacy and potency of β-AR-induced stimulation of Ca^{2+}-transients. Notably, at baseline and at low ISO concentrations, contractile parameters were normal (Suppl. Fig. 8). However, the *in vitro* findings regarding force development did not entirely recapitulate the actual phenotype of PDE2-TG mice. Our *in vivo* data clearly demonstrate that PDE2 overexpression was associated with a normal contractile reserve and rather improved contraction force. This was even maintained when heart rate was reduced to an identical level (332±15 *vs*. 306±8 bpm) induced by acute β-blockade (Fig. 2 D-F) indicating that the lower basal heart rate per se e.g. via augmented filling in diastole cannot completely explain the hypercontractile phenotype. Despite lower PLB-phosphorylation, SR load did not appear affected in PDE2-TG. Longer diastolic intervals and the reduced Ca^{2+} leak may therefore be sufficient for maintaining adequate SR Ca^{2+} filling and preservation of cardiac function *in vivo*, even in the presence of reduced SERCA activity[48]. In summary,

PDE2 overexpression offers a potential dual protection by limiting heart rate without affecting chronotropic adaptation and by attenuating ventricular SR Ca^{2+}-release with the benefit of lower arrhythmia susceptibility. The effect of PDE2 overexpression is therefore similar to β-blocker treatment but without depression of contractile performance.

PDE2 in cardiac remodeling

A very recent publication proposed that in context of cardiac remodeling processes, chronic inhibition of PDE2 leads to a reduction of pathological hypertrophic growth[49]. While this contradicts our earlier finding that adenoviral overexpression of PDE2 antagonizes β-AR induced cellular hypertrophy [29, 50], we observed a small but not significant increase in cardiac size in PDE2-TG mice as compared to WT (Fig. 2G, 3C). Therefore, we cannot completely rule out a minor increase of heart size due to PDE2 overexpression. Consistently, heart weight was also ~10% higher in PDE2-TG mice after MI compared to WT (Suppl. Fig. 11). However, preservation of cardiac function and size up to an advanced age (Fig. 3) strongly argues against pathological hypertrophy. Moreover, we offer proof that high abundance of PDE2 significantly protects against acute and chronic β-AR stress and maintains contractile function after MI.

Potential limitations

A general limitation of transgenic "overexpressors" is potential spill over within subcellular compartments, where the protein of interest may be not physiologically located. This is even more critical when examining PDEs, which control highly compartmentalized cAMP pools and redistribution phenomena under pathological conditions have been reported[51, 52]. Despite designing our experiments following general recommendations for state-of-the-art phenotyping of transgenic mice[35], we are not able to fully exclude artificial compartmentation effects. However, the specificity of the phenotype and its striking similarities to *in vivo* studies of endogenous PDE2 from mice and larger animals offers a valid approach for analyzing the pathophysiological role of PDE2 in heart function. A second limitation is that the role played by each PDE isoform varies among mammalian species[53, 54] and accordingly, our results may not recapitulate the situation in humans in all details.

Clinical perspective: PDE2 as a downstream target of cGMP pools

The current therapeutic strategies for HF and prevention of sudden cardiac death are only moderately effective. Despite all efforts, a lack of understanding of the pathophysiological mechanisms underlying HF and arrhythmias has hindered the development of more effective, rational therapeutic approaches. Recently, the publication of the PARADIGM-HF trial, which demonstrated the successful introduction of the compound LCZ696 (a combination of a standard Angiotesin-II-receptor-1 blocker and an inhibitor of the NP-degrading enzyme neprilysin), has once again shifted the enhancement of cGMP-signaling into the focus of HF therapy. One remarkable result of the study was a significant protection from sudden cardiac death[55, 56]. The importance of the NP signaling pathway was further emphasized in a study by the Kass group showing that the inhibition of cGMP-degrading PDE9 protects against HF progression by specifically targeting the ANP/BNP-coupled cGMP pool[16, 57]. PDE2 is a central component of the cGMP/cAMP crosstalk and as our study demonstrates effectively protects against ventricular arrhythmia during excessive sympathetic stress and improved ventricular function after a severe cardiac insult. It may therefore constitute an up to now unconsidered link between ANP/BNP-coupled cGMP enhancement and the protection against toxic sympathetic effects by acting as a cGMP controlled intracellular sympathetic blockade. Thus, PDE2 is worth being considered a key element in recent encouraging therapeutic approaches and accordingly its direct activation may offer an alternative strategy in a promising new field of HF therapy.

Acknowledgments: We wish to thank Roland Blume, Ursel Leonard, Daniela Wolter, Marcel Zoremba (University Medical Center Göttingen), and Stefano Gaburro (DSI) for their technical support. Further, Florence Lefebvre for cell isolation, and Pauline Robert and Valérie Domergue-Dupont (Animal core facility, University of Paris-Sud, UMS-IPSIT) for handling and genotyping of mice.

Funding sources: This study was supported by Deutsche Forschungsgemeinschaft Grants DFG EL 270/7-1 (to A. El-Armouche), DFG WA 2586/4-1 (to M. Wagner), SFB 1002 (to A. El-Armouche), and IRTG 1816 (to C. Vettel, and A. El-Armouche), by the Investment for the Future program ANR-11-IDEX-0003-01 within the LABEX ANR-10-LABX-0033 (to R. Fischmeister and M. Lindner), the Fondation Lefoulon-Delalande (to S. Karam) and the German Centre for Cardiovascular Research.

Disclosures: None

References

1. Cohn JN, Levine TB, Olivari MT, Garberg V, Lura D, Francis GS, Simon AB, Rector T. Plasma norepinephrine as a guide to prognosis in patients with chronic congestive heart failure. *The New England journal of medicine*. 1984;311:819-823
2. Tomaselli GF, Zipes DP. What causes sudden death in heart failure? *Circulation research*. 2004;95:754-763
3. Coronel R, Wilders R, Verkerk AO, Wiegerinck RF, Benoist D, Bernus O. Electrophysiological changes in heart failure and their implications for arrhythmogenesis. *Biochim Biophys Acta*. 2013;1832:2432-2441
4. Fox K, Ford I, Steg PG, Tendera M, Robertson M, Ferrari R, investigators B. Heart rate as a prognostic risk factor in patients with coronary artery disease and left-ventricular systolic dysfunction (beautiful): A subgroup analysis of a randomised controlled trial. *Lancet*. 2008;372:817-821
5. Bilchick KC, Berger RD. Heart rate variability. *Journal of cardiovascular electrophysiology*. 2006;17:691-694
6. Bristow MR, Ginsburg R, Minobe W, Cubicciotti RS, Sageman WS, Lurie K, Billingham ME, Harrison DC, Stinson EB. Decreased catecholamine sensitivity and beta-adrenergic-receptor density in failing human hearts. *The New England journal of medicine*. 1982;307:205-211
7. Nikolaev VO, Moshkov A, Lyon AR, Miragoli M, Novak P, Paur H, Lohse MJ, Korchev YE, Harding SE, Gorelik J. Beta2-adrenergic receptor redistribution in heart failure changes camp compartmentation. *Science*. 2010;327:1653-1657
8. El-Armouche A, Eschenhagen T. Beta-adrenergic stimulation and myocardial function in the failing heart. *Heart failure reviews*. 2009;14:225-241
9. Tilley DG, Rockman HA. Role of beta-adrenergic receptor signaling and desensitization in heart failure: New concepts and prospects for treatment. *Expert review of cardiovascular therapy*. 2006;4:417-432
10. Bristow MR. Pathophysiologic and pharmacologic rationales for clinical management of chronic heart failure with beta-blocking agents. *The American journal of cardiology*. 1993;71:12C-22C
11. Effect of metoprolol cr/xl in chronic heart failure: Metoprolol cr/xl randomised intervention trial in congestive heart failure (merit-hf). *Lancet*. 1999;353:2001-2007
12. Flannery G, Gehrig-Mills R, Billah B, Krum H. Analysis of randomized controlled trials on the effect of magnitude of heart rate reduction on clinical outcomes in patients with systolic chronic heart failure receiving beta-blockers. *The American journal of cardiology*. 2008;101:865-869
13. Swedberg K, Komajda M, Bohm M, Borer JS, Ford I, Dubost-Brama A, Lerebours G, Tavazzi L, Investigators S. Ivabradine and outcomes in chronic heart failure (shift): A randomised placebo-controlled study. *Lancet*. 2010;376:875-885
14. Walker MJ, Curtis MJ, Hearse DJ, Campbell RW, Janse MJ, Yellon DM, Cobbe SM, Coker SJ, Harness JB, Harron DW, et al. The lambeth conventions: Guidelines for the study of arrhythmias in ischaemia infarction, and reperfusion. *Cardiovascular research*. 1988;22:447-455
15. Lee DI, Vahebi S, Tocchetti CG, Barouch LA, Solaro RJ, Takimoto E, Kass DA. Pde5a suppression of acute beta-adrenergic activation requires modulation of myocyte beta-3 signaling coupled to pkg-mediated troponin i phosphorylation. *Basic Res Cardiol*. 2010;105:337-347
16. Lee DI, Zhu G, Sasaki T, Cho GS, Hamdani N, Holewinski R, Jo SH, Danner T, Zhang M, Rainer PP, Bedja D, Kirk JA, Ranek MJ, Dostmann WR, Kwon C, Margulies KB, Van Eyk JE, Paulus WJ, Takimoto E, Kass DA. Phosphodiesterase 9a controls nitric-oxide-independent cgmp and hypertrophic heart disease. *Nature*. 2015;519:472-476
17. Nagayama T, Hsu S, Zhang M, Koitabashi N, Bedja D, Gabrielson KL, Takimoto E, Kass DA. Sildenafil stops progressive chamber, cellular, and molecular remodeling

and improves calcium handling and function in hearts with pre-existing advanced hypertrophy caused by pressure overload. *J Am Coll Cardiol*. 2009;53:207-215
18. Wang H, Kohr MJ, Traynham CJ, Ziolo MT. Phosphodiesterase 5 restricts nos3/soluble guanylate cyclase signaling to l-type ca2+ current in cardiac myocytes. *J Mol Cell Cardiol*. 2009;47:304-314
19. Mika D, Leroy J, Vandecasteele G, Fischmeister R. Pdes create local domains of camp signaling. *J Mol Cell Cardiol*. 2012;52:323-329
20. Martinez SE, Wu AY, Glavas NA, Tang XB, Turley S, Hol WG, Beavo JA. The two gaf domains in phosphodiesterase 2a have distinct roles in dimerization and in cgmp binding. *Proc Natl Acad Sci U S A*. 2002;99:13260-13265
21. Wu AY, Tang XB, Martinez SE, Ikeda K, Beavo JA. Molecular determinants for cyclic nucleotide binding to the regulatory domains of phosphodiesterase 2a. *J Biol Chem*. 2004;279:37928-37938
22. Martinez SE, Beavo JA, Hol WG. Gaf domains: Two-billion-year-old molecular switches that bind cyclic nucleotides. *Molecular interventions*. 2002;2:317-323
23. Dittrich M, Jurevicius J, Georget M, Rochais F, Fleischmann B, Hescheler J, Fischmeister R. Local response of l-type ca(2+) current to nitric oxide in frog ventricular myocytes. *J Physiol*. 2001;534:109-121
24. Vandecasteele G, Verde I, Rucker-Martin C, Donzeau-Gouge P, Fischmeister R. Cyclic gmp regulation of the l-type ca(2+) channel current in human atrial myocytes. *J Physiol*. 2001;533:329-340
25. Mongillo M, Tocchetti CG, Terrin A, Lissandron V, Cheung YF, Dostmann WR, Pozzan T, Kass DA, Paolocci N, Houslay MD, Zaccolo M. Compartmentalized phosphodiesterase-2 activity blunts beta-adrenergic cardiac inotropy via an no/cgmp-dependent pathway. *Circulation research*. 2006;98:226-234
26. MacFarland RT, Zelus BD, Beavo JA. High concentrations of a cgmp-stimulated phosphodiesterase mediate anp-induced decreases in camp and steroidogenesis in adrenal glomerulosa cells. *J Biol Chem*. 1991;266:136-142
27. Ding B, Abe J, Wei H, Huang Q, Walsh RA, Molina CA, Zhao A, Sadoshima J, Blaxall BC, Berk BC, Yan C. Functional role of phosphodiesterase 3 in cardiomyocyte apoptosis: Implication in heart failure. *Circulation*. 2005;111:2469-2476
28. Abi-Gerges A, Richter W, Lefebvre F, Mateo P, Varin A, Heymes C, Samuel JL, Lugnier C, Conti M, Fischmeister R, Vandecasteele G. Decreased expression and activity of camp phosphodiesterases in cardiac hypertrophy and its impact on beta-adrenergic camp signals. *Circulation research*. 2009;105:784-792
29. Mehel H, Emons J, Vettel C, Wittkopper K, Seppelt D, Dewenter M, Lutz S, Sossalla S, Maier LS, Lechene P, Leroy J, Lefebvre F, Varin A, Eschenhagen T, Nattel S, Dobrev D, Zimmermann WH, Nikolaev VO, Vandecasteele G, Fischmeister R, El-Armouche A. Phosphodiesterase-2 is up-regulated in human failing hearts and blunts beta-adrenergic responses in cardiomyocytes. *J Am Coll Cardiol*. 2013;62:1596-1606
30. Subramaniam A, Jones WK, Gulick J, Wert S, Neumann J, Robbins J. Tissue-specific regulation of the alpha-myosin heavy chain gene promoter in transgenic mice. *J Biol Chem*. 1991;266:24613-24620
31. Borner S, Schwede F, Schlipp A, Berisha F, Calebiro D, Lohse MJ, Nikolaev VO. Fret measurements of intracellular camp concentrations and camp analog permeability in intact cells. *Nature protocols*. 2011;6:427-438
32. Klarenbeek J, Goedhart J, van Batenburg A, Groenewald D, Jalink K. Fourth-generation epac-based fret sensors for camp feature exceptional brightness, photostability and dynamic range: Characterization of dedicated sensors for flim, for ratiometry and with high affinity. *PloS one*. 2015;10:e0122513
33. Leroy J, Richter W, Mika D, Castro LR, Abi-Gerges A, Xie M, Scheitrum C, Lefebvre F, Schittl J, Mateo P, Westenbroek R, Catterall WA, Charpentier F, Conti M, Fischmeister R, Vandecasteele G. Phosphodiesterase 4b in the cardiac l-type ca(2)(+) channel complex regulates ca(2)(+) current and protects against ventricular arrhythmias in mice. *The Journal of clinical investigation*. 2011;121:2651-2661

34. Masood A, Huang Y, Hajjhussein H, Xiao L, Li H, Wang W, Hamza A, Zhan CG, O'Donnell JM. Anxiolytic effects of phosphodiesterase-2 inhibitors associated with increased cgmp signaling. *The Journal of pharmacology and experimental therapeutics*. 2009;331:690-699
35. Davis J, Maillet M, Miano JM, Molkentin JD. Lost in transgenesis: A user's guide for genetically manipulating the mouse in cardiac research. *Circulation research*. 2012;111:761-777
36. Hayano J, Sakakibara Y, Yamada A, Yamada M, Mukai S, Fujinami T, Yokoyama K, Watanabe Y, Takata K. Accuracy of assessment of cardiac vagal tone by heart rate variability in normal subjects. *The American journal of cardiology*. 1991;67:199-204
37. Schweizer PA, Duhme N, Thomas D, Becker R, Zehelein J, Draguhn A, Bruehl C, Katus HA, Koenen M. Camp sensitivity of hcn pacemaker channels determines basal heart rate but is not critical for autonomic rate control. *Circulation. Arrhythmia and electrophysiology*. 2010;3:542-552
38. Wittkopper K, Fabritz L, Neef S, Ort KR, Grefe C, Unsold B, Kirchhof P, Maier LS, Hasenfuss G, Dobrev D, Eschenhagen T, El-Armouche A. Constitutively active phosphatase inhibitor-1 improves cardiac contractility in young mice but is deleterious after catecholaminergic stress and with aging. *The Journal of clinical investigation*. 2010;120:617-626
39. Neef S, Maier LS. Novel aspects of excitation-contraction coupling in heart failure. *Basic Res Cardiol*. 2013;108:360
40. Respress JL, van Oort RJ, Li N, Rolim N, Dixit SS, deAlmeida A, Voigt N, Lawrence WS, Skapura DG, Skardal K, Wisloff U, Wieland T, Ai X, Pogwizd SM, Dobrev D, Wehrens XH. Role of ryr2 phosphorylation at s2814 during heart failure progression. *Circulation research*. 2012;110:1474-1483
41. van Oort RJ, McCauley MD, Dixit SS, Pereira L, Yang Y, Respress JL, Wang Q, De Almeida AC, Skapura DG, Anderson ME, Bers DM, Wehrens XH. Ryanodine receptor phosphorylation by calcium/calmodulin-dependent protein kinase ii promotes life-threatening ventricular arrhythmias in mice with heart failure. *Circulation*. 2010;122:2669-2679
42. DiFrancesco D. The role of the funny current in pacemaker activity. *Circulation research*. 2010;106:434-446
43. Lakatta EG, Maltsev VA, Vinogradova TM. A coupled system of intracellular ca2+ clocks and surface membrane voltage clocks controls the timekeeping mechanism of the heart's pacemaker. *Circulation research*. 2010;106:659-673
44. Lyashkov AE, Vinogradova TM, Zahanich I, Li Y, Younes A, Nuss HB, Spurgeon HA, Maltsev VA, Lakatta EG. Cholinergic receptor signaling modulates spontaneous firing of sinoatrial nodal cells via integrated effects on pka-dependent ca(2+) cycling and i(kach). *American journal of physiology. Heart and circulatory physiology*. 2009;297:H949-959
45. Hua R, Adamczyk A, Robbins C, Ray G, Rose RA. Distinct patterns of constitutive phosphodiesterase activity in mouse sinoatrial node and atrial myocardium. *PloS one*. 2012;7:e47652
46. Alig J, Marger L, Mesirca P, Ehmke H, Mangoni ME, Isbrandt D. Control of heart rate by camp sensitivity of hcn channels. *Proc Natl Acad Sci U S A*. 2009;106:12189-12194
47. Bers DM. Cardiac sarcoplasmic reticulum calcium leak: Basis and roles in cardiac dysfunction. *Annual review of physiology*. 2014;76:107-127
48. Neef S, Dybkova N, Sossalla S, Ort KR, Fluschnik N, Neumann K, Seipelt R, Schondube FA, Hasenfuss G, Maier LS. Camkii-dependent diastolic sr ca2+ leak and elevated diastolic ca2+ levels in right atrial myocardium of patients with atrial fibrillation. *Circulation research*. 2010;106:1134-1144
49. Zoccarato A, Surdo NC, Aronsen JM, Fields LA, Mancuso L, Dodoni G, Stangherlin A, Livie C, Jiang H, Sin YY, Gesellchen F, Terrin A, Baillie GS, Nicklin SA, Graham D, Szabo-Fresnais N, Krall J, Vandeput F, Movsesian M, Furlan L, Corsetti V, Hamilton

GM, Lefkimmiatis K, Sjaastad I, Zaccolo M. Cardiac hypertrophy is inhibited by a local pool of camp regulated by phosphodiesterase 2. *Circulation research*. 2015

50. Wagner M, Mehel H, Fischmeister R, El-Armouche A. Phosphodiesterase 2: Anti-adrenergic friend or hypertrophic foe in heart disease? *Naunyn-Schmiedeberg's archives of pharmacology*. 2016
51. Perera RK, Sprenger JU, Steinbrecher JH, Hubscher D, Lehnart SE, Abesser M, Schuh K, El-Armouche A, Nikolaev VO. Microdomain switch of cgmp-regulated phosphodiesterases leads to anp-induced augmentation of beta-adrenoceptor-stimulated contractility in early cardiac hypertrophy. *Circulation research*. 2015;116:1304-1311
52. Zhang M, Takimoto E, Lee DI, Santos CX, Nakamura T, Hsu S, Jiang A, Nagayama T, Bedja D, Yuan Y, Eaton P, Shah AM, Kass DA. Pathological cardiac hypertrophy alters intracellular targeting of phosphodiesterase type 5 from nitric oxide synthase-3 to natriuretic peptide signaling. *Circulation*. 2012;126:942-951
53. Fischmeister R, Castro LR, Abi-Gerges A, Rochais F, Jurevicius J, Leroy J, Vandecasteele G. Compartmentation of cyclic nucleotide signaling in the heart: The role of cyclic nucleotide phosphodiesterases. *Circulation research*. 2006;99:816-828
54. Zaccolo M, Movsesian MA. Camp and cgmp signaling cross-talk: Role of phosphodiesterases and implications for cardiac pathophysiology. *Circulation research*. 2007;100:1569-1578
55. McMurray JJ, Packer M, Desai AS, Gong J, Lefkowitz MP, Rizkala AR, Rouleau J, Shi VC, Solomon SD, Swedberg K, Zile MR, Committees P-H, Investigators. Dual angiotensin receptor and neprilysin inhibition as an alternative to angiotensin-converting enzyme inhibition in patients with chronic systolic heart failure: Rationale for and design of the prospective comparison of arni with acei to determine impact on global mortality and morbidity in heart failure trial (paradigm-hf). *European journal of heart failure*. 2013;15:1062-1073
56. McMurray JJ, Packer M, Desai AS, Gong J, Lefkowitz MP, Rizkala AR, Rouleau JL, Shi VC, Solomon SD, Swedberg K, Zile MR, Investigators P-H, Committees. Angiotensin-neprilysin inhibition versus enalapril in heart failure. *The New England journal of medicine*. 2014;371:993-1004
57. Kuhn M. Cardiology: A big-hearted molecule. *Nature*. 2015;519:416-417

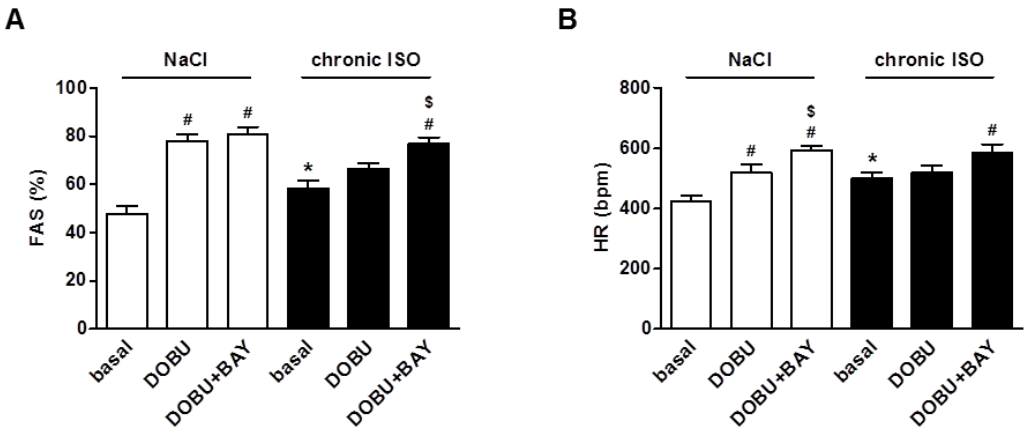

Figure 1. PDE2 regulates heart rate and blunts β-AR-induced inotropy in animals chronically treated with ISO. Effect of PDE2 inhibition in mice exposed to chronic ISO infusions for 7 d (30 mg/kg*d) or treated with vehicle (0.9% NaCl). Animals were anaesthetized and monitored by echocardiography under basal conditions, 2-7 min after dobutamine (10 mg/kg i.p., DOBU) injection and 10 min after application of the PDE2 inhibitor BAY 60-7550 (3 mg/kg i.p., BAY) on top of DOBU (DOBU+BAY). (A) Fractional area shortening (FAS). (B) Heart rate (HR); n=7-8 for each group. Statistical significance was determined by one-way ANOVA followed by Newman-Keuls multiple comparison test. *$p<0.05$ *vs.* NaCl, $^{\#}p<0.05$ *vs.* respective basal, and $^{\$}p<0.05$ *vs.* DOBU.

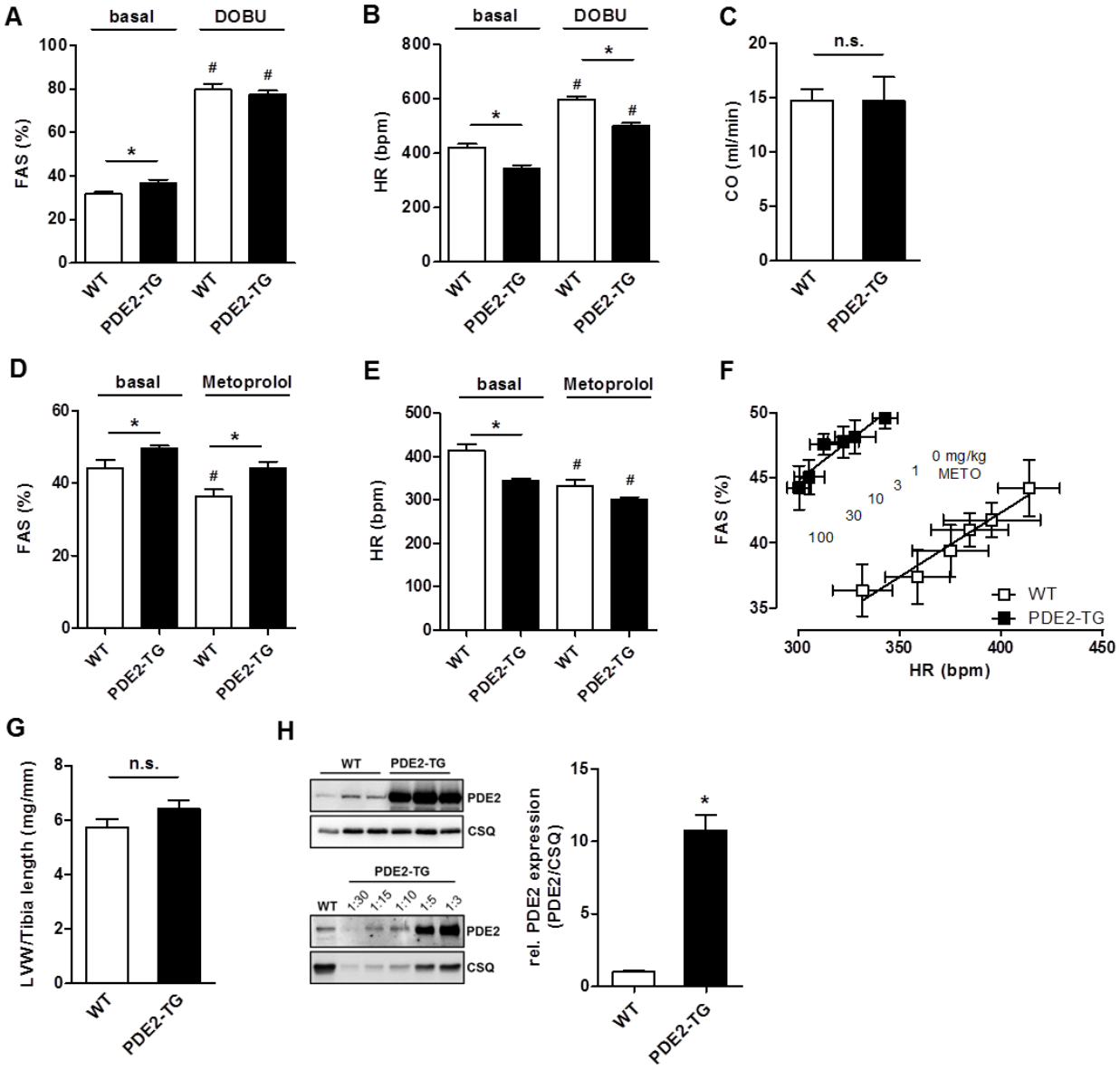

Figure 2. Higher basal contractility and lower heart rate in PDE2-TG. Echocardiographic determination of fractional area shortening (FAS, A), heart rate cardiac (HR, B) and output (CO, C), and in anaesthetized 2 month old mice. Animals were treated with 10 mg/kg dobutamine (DOBU, i.p.) 2 min prior to measurements when indicated; n=7-9 for each group. Effect of metoprolol (100 mg/kg, i.p.) on (D) FAS and (E) HR in anaesthetized animals. (G) Correlation between the reduction of FAS and HR in the presence of increasing metoprolol doses (METO 0, 1, 3, 10, 30 and 100 mg/kg); n=5 for each group. (G) Left ventricular weight (LVW) calculated from the echocardiographic data and normalized to tibia length. (H) Lysates prepared from ventricular myocardium were analyzed by immunoblot with the indicated specific antibodies. PDE2 expression was normalized to calsequestrin (CSQ) and given relative to WT. (E) Representative immunoblots and (F) quantification; n=7-9 for each group. Statistical significance was determined by One-way ANOVA followed by Newman-Keuls multiple comparison test (A, B, D, E) and Student's *t*-test to compare the two genotypes on basal level (A-E, G,H). *p<0.05 *vs*. WT, #p<0.05 *vs.* respective basal.

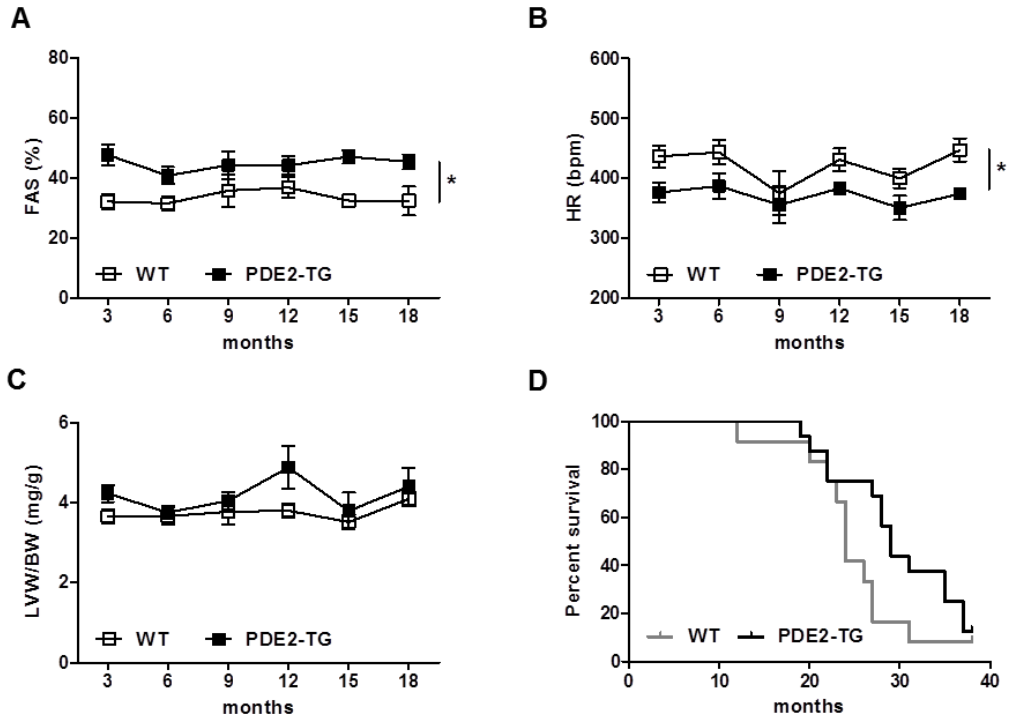

Figure 3. Preserved phenotype of higher basal contractility and lower heart rate in elderly PDE2-TG. Echocardiographic determination of fractional area shortening (FAS, A), and heart rate (HR, B) in anaesthetized 3-18 month old mice. (C) Left ventricular weight (LVW) was calculated from the echocardiographic data and normalized to body weight (BW); n=6 for each group. Statistical significance was determined by Two-way ANOVA. *p<0.05 *vs*. WT. (D) Longevity study of WT (n=12) and PDE2-TG (n=16). The study was terminated after 38 months. Average life span of WT=24 and PDE2-TG=29 months.

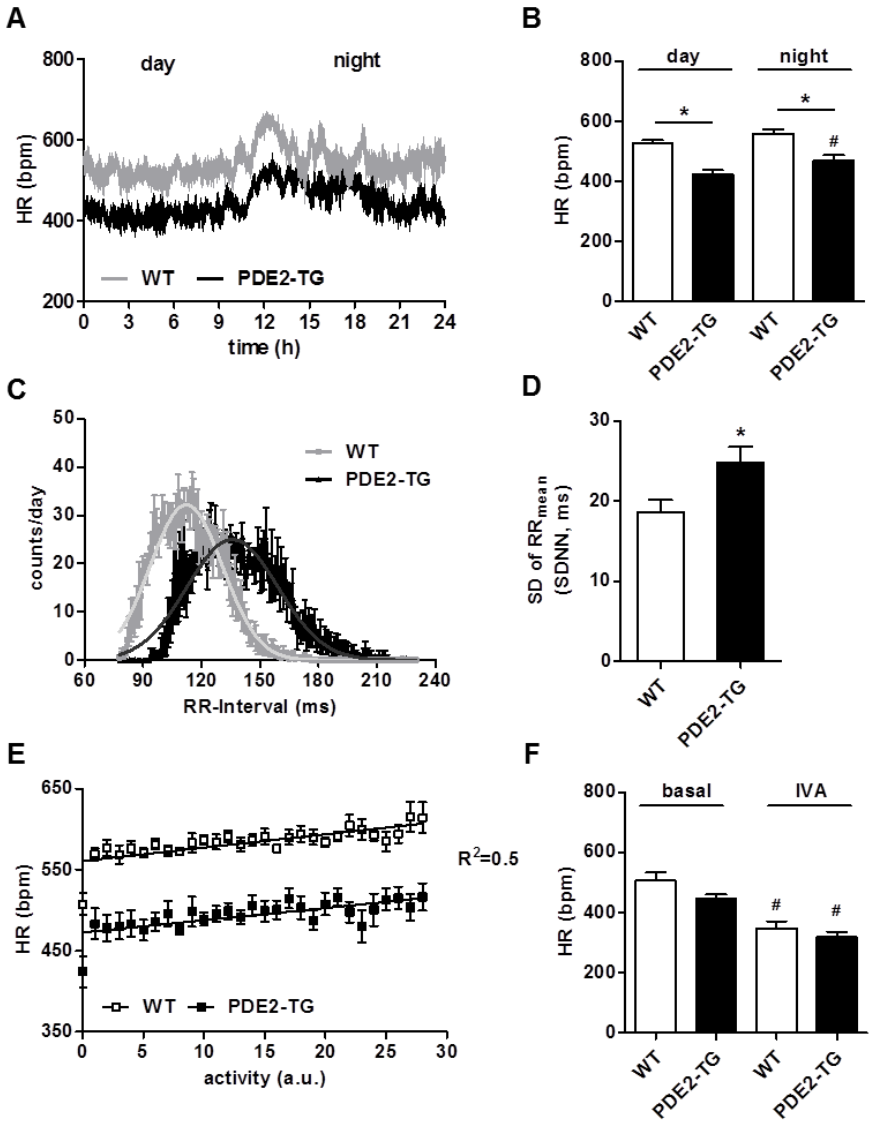

Figure 4. PDE2 transgenic mice show higher heart rate variability and normal chronotropic adaptation. Animals (n=4-5 per genotype) were monitored by ECG-telemetry for a period of 72 h to calculate average changes in heart rate (HR) and heart rate variability of a 24 h cycle. Frequencies and activity were tracked as averages of 1 min intervals. (A) Average circadian changes in heart rate over a period of 24 h. (B) Average heart rate during day and night periods. (C) Heart rate variability given as occurrence of RR-intervals during one 24 h recording with Gaussian distribution curve calculated for each group. (D) Standard derivation of average RR-intervals (SDNN). (E) Correlation between heart rate and activity. (F) Average HR over a period of 20 min prior (0-20 min) and after ivabradine (IVA, 5 mg/kg, i.p.) injection (10-30 min). Statistical significance was determined by one-way ANOVA followed by Newman-Keuls multiple comparison test and Student's *t*-test to compare the two genotypes (D). *p<0.05 *vs*. WT, #p<0.05 *vs*. day (B) or respective basal (F).

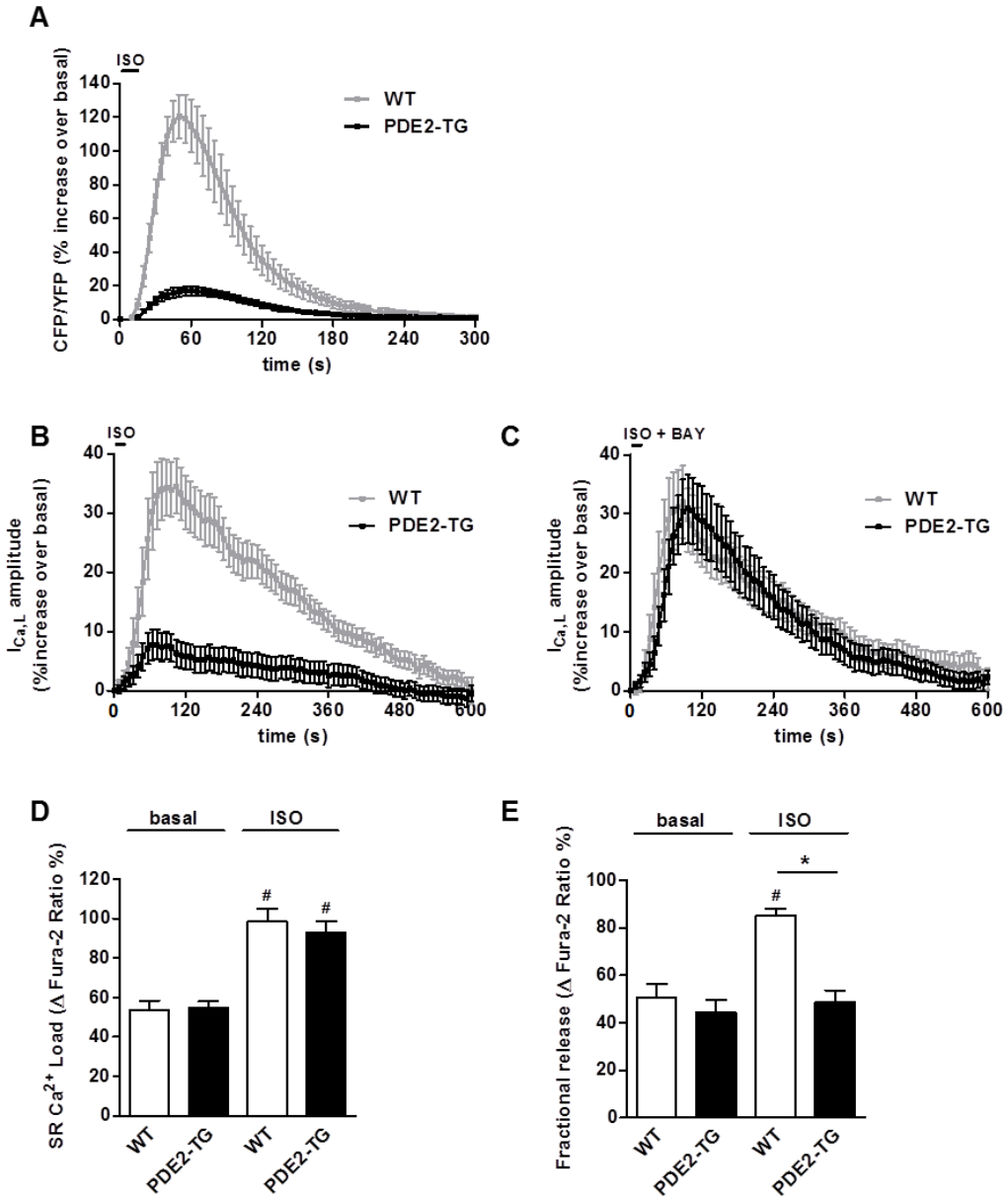

Figure 5. Ventricular myocytes from PDE2-TG mice show reduced β-AR-response, but normal SR Ca^{2+} load. (A) Normalized average time course of $[cAMP]_i$ in response to a 15 s application of ISO (30 nmol/L) in WT and PDE2-TG ventricular myocytes infected with an adenovirus expressing the FRET-based cAMP probe Epac-S^{H187}; n=3 animals/genotype with 11-13 cell in each group. (B, C) Normalized average time course of $I_{Ca,L}$ amplitude following ISO pulse stimulation (30 nmol/L, 15 s) in the absence (B) or presence (C) of PDE2 inhibitor BAY 60-7550 (100 nmol/L). The cells were depolarized every 8 s from -50 to 0 mV during 400 ms; n=3 animals/genotype with 10-19 cell in each group. (D) Mean amplitude of SR Ca^{2+} load in the presence or absence of ISO measured as the change in Fura-2 ratio after rapid application of caffeine (10 mmol/L). (E, F) SR Ca^{2+} load and fractional release measured in Fura-2 loaded adult mouse ventricular myocytes paced at 1 Hz, in the presence or absence of ISO (100 nmol/L) (E) Mean fractional Ca^{2+} release in control or ISO calculated as the ratio of Ca^{2+} transient amplitude divided by caffeine-induced response; n=2-3 animals/genotype with 7-11 cells in each group. Statistical significance was determined by One-way ANOVA followed by Newman-Keuls multiple comparison test. *p<0.05 *vs*. WT, $^{\#}$p<0.05 *vs*. respective basal.

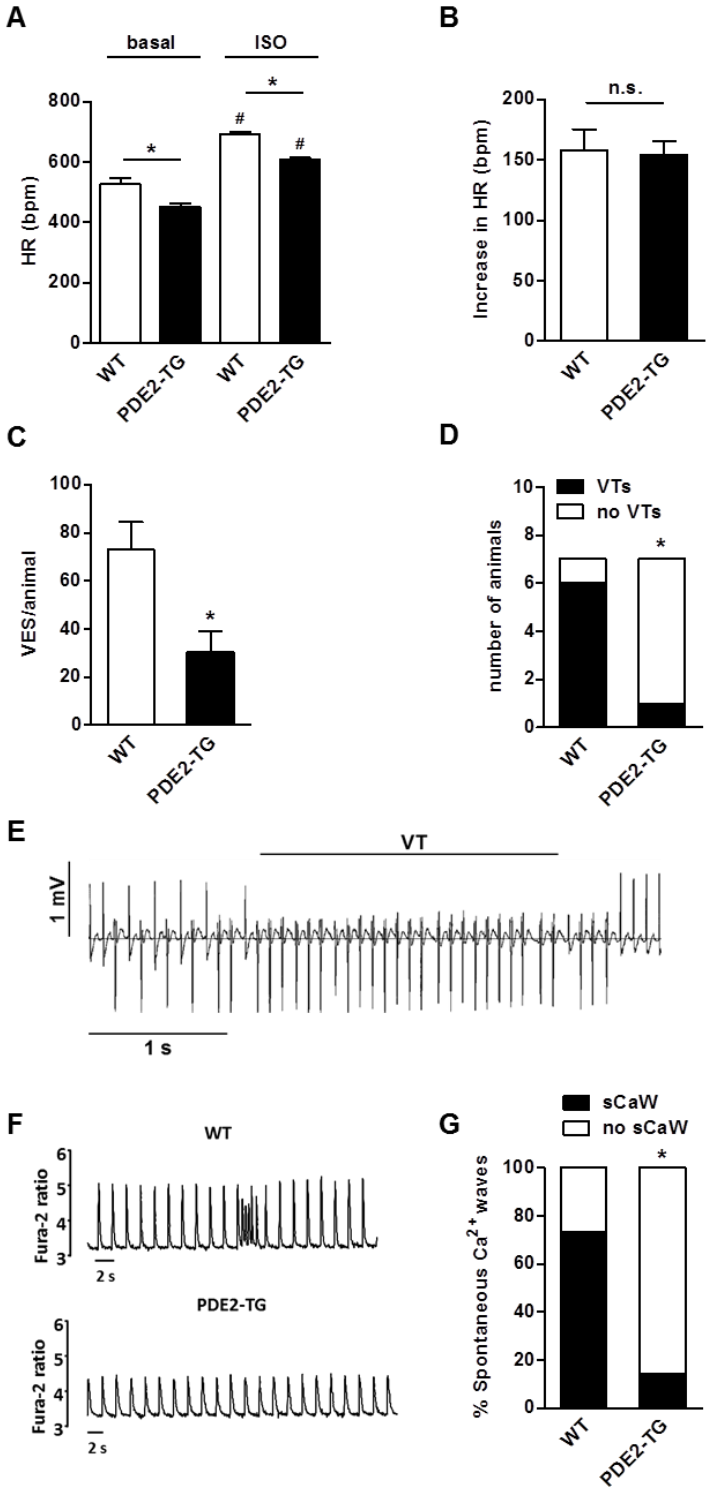

Figure 6. PDE2 transgenic mice show the same absolute increase in heart rate after β-AR stimulation, but lower susceptibility to arrhythmic events. Heart rate was monitored after double ISO injection (2 mg/kg, i.p.; time interval between injections: 30 min) and analyzed for ventricular extra systoles (VES), salvos and ventricular tachycardia (VT) over a period of 90 min after the first application; n=7. (A) ISO-induced increase in heat rate (HR) calculated as an average of 5 s intervals. (B) Absolute increase over basal heart rate. (C) Total number of VES per animal. (D) Number of animals with VTs; n=7. (E) Representative trace of a WT animal showing VTs; with bigeminy (alternations of sinus beat and VES) before onset of VT. (F, G) Effect of PDE2 overexpression on spontaneous Ca^{2+} waves (sCaW) in mouse

ventricular cells. (F) Representative traces of Ca^{2+} transients in Fura-2 loaded mouse ventricular cells isolated from WT or PDE2-TG mice paced at 0.5 Hz in the presence of 100 nmol/L ISO. (G) Percent of cells with sCaW in WT and PDE2-TG mice after ISO-treatment; n=3-4 animals/genotype with a total of 16-22 cells in each group. Statistical significance was determined by One-way ANOVA followed by Newman-Keuls multiple comparison test (A), Student's *t*-test to compare the two genotypes (B, C) and Fisher's exact test (D, G) to compare occurrence of events. *$p<0.05$ *vs*. WT, $^{\#}p<0.05$ *vs*. respective basal.

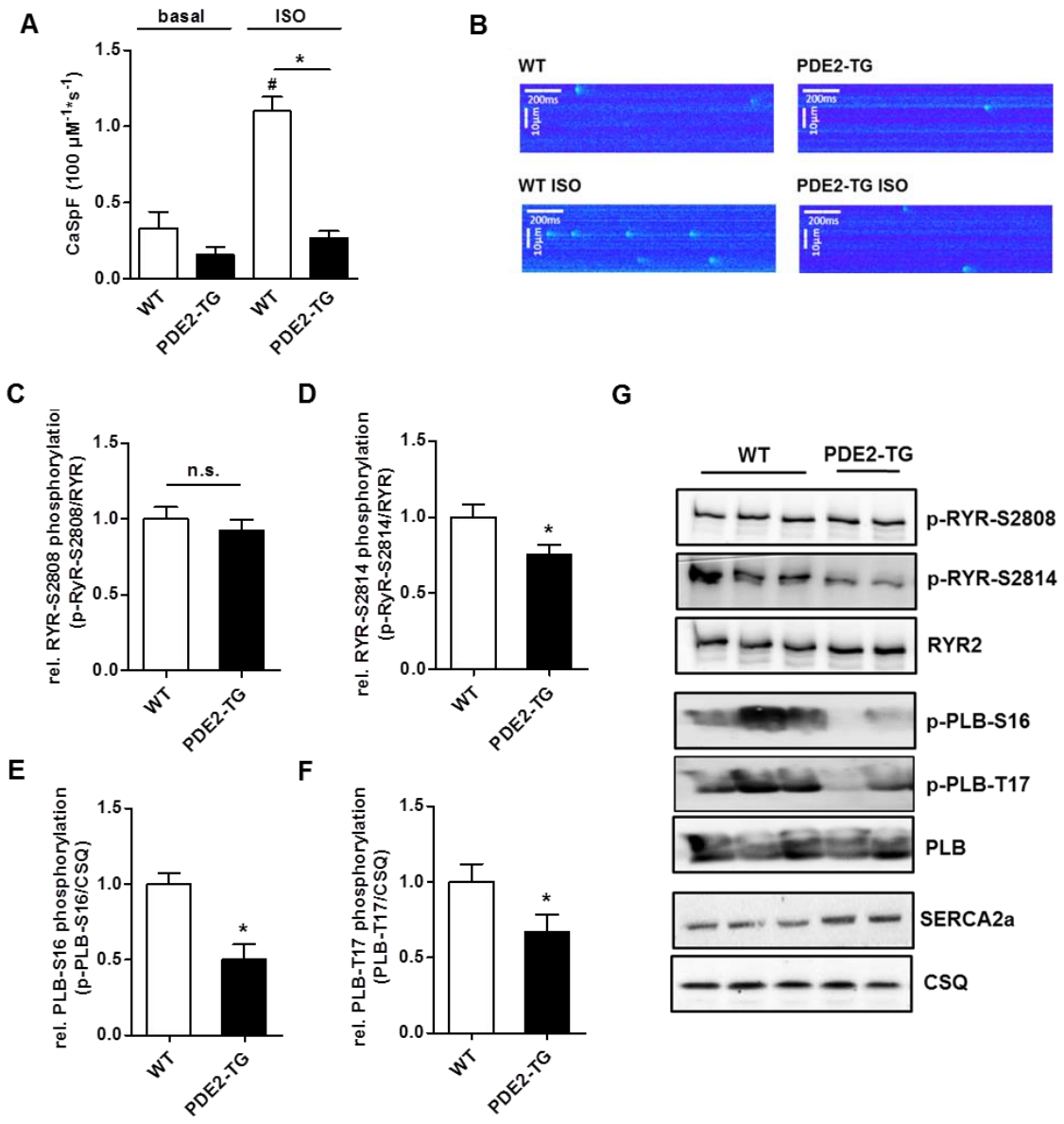

Figure 7. PDE2 transgenic mice show reduction in Ca^{2+} leak and phosphorylation of Ca^{2+} handling SR proteins in ventricular myocardium. (A, B) Ventricular myocytes were loaded with Fluo-3 AM and monitored for Ca^{2+}-sparks by laser scanning confocal microscopy under basal conditions and after stimulation with 100 nmol/L ISO. (A) Quantification of Ca^{2+}-spark frequency (CaSpF) normalized to cell width and scan rate. (B) Representative original recordings, n=4 animals/genotype. (C-G) Lysates prepared from ventricular myocardium were analyzed by immunoblot with the indicated specific antibodies. Protein phosphorylation was normalized to the respective total protein. (C-F) Quantification and (G) representative immunoblots showing additionally the expression levels of sarcolemma Ca^{2+} ATPase 2a (SERCA2a) and calsequestrin (CSQ); n=7-8 for each group. Statistical significance was determined by One-way ANOVA followed by Newman-Keuls multiple comparison test and Student's t-test to compare the two genotypes. *p<0.05 *vs*. WT, $^{\#}$p<0.05 *vs*. respective basal.

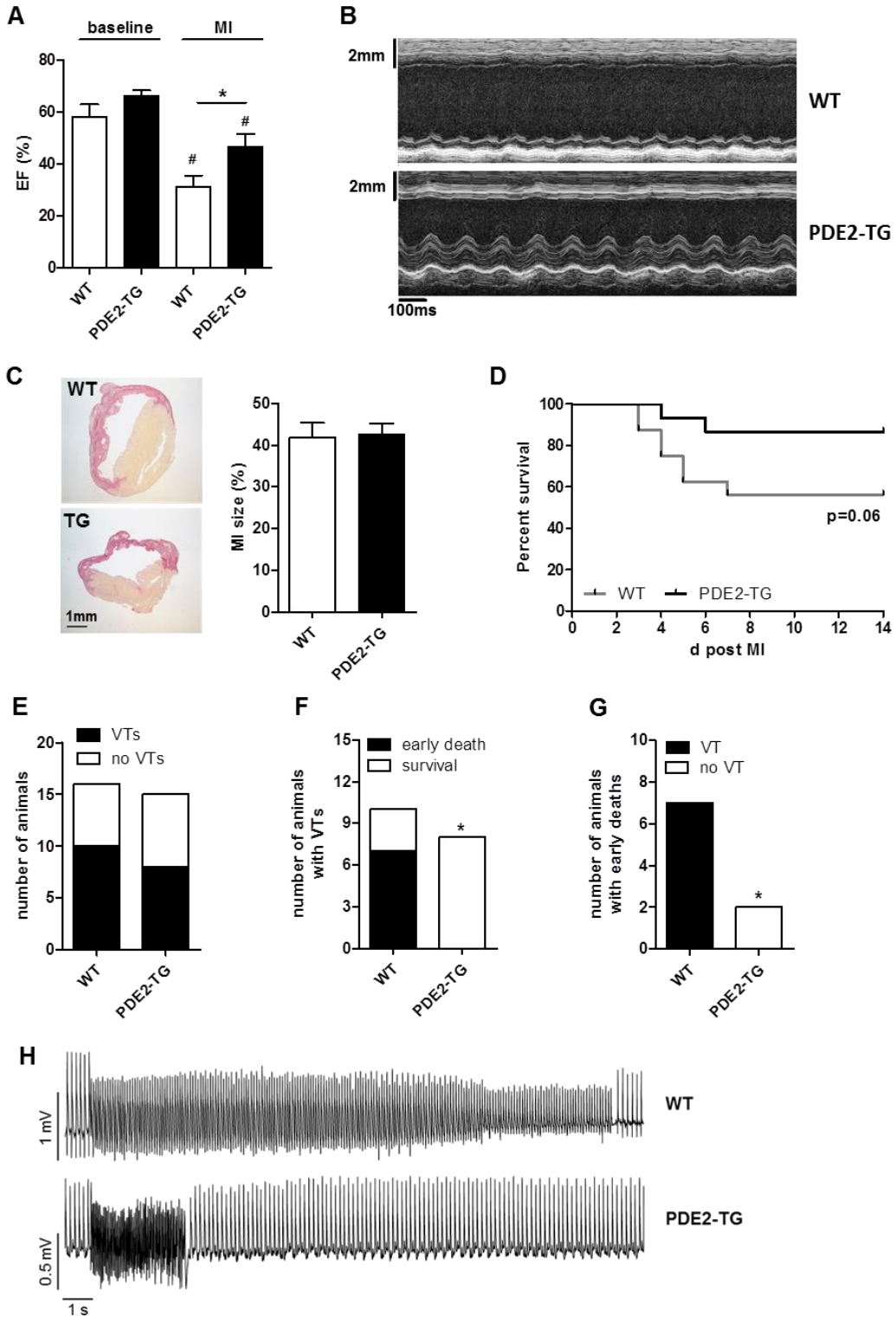

Figure 8. PDE2-TG are protected from early death, sustained arrhythmias and decline of heart function after myocardial infarct (MI). (A) Ejection fraction calculated from echocardiographic analysis prior MI (baseline) and at day 14 post MI. (B) Representative M-Mode trace from infarcted area taken 14 d post MI. (C) *Left panel:* Representative Sirius Red staining of heart sections prepared from surviving animals at day 14; *right panel:* quantification of infarct size given as % of total tissue area. (D) % of surviving animals. Study was terminated 14 d post MI. (E, F, G) Analysis of ventricular tachycardia (VT) during the first

40 h post MI and association with early death events. (~~F~~H) Representative ECG-traces showing a 17 s lasting VT in WT and 4 s in TG animals. Statistical significance was determined by One-way ANOVA followed by Newman-Keuls multiple comparison test (A), Long rank test (B), and Fischer's exact test (F, G). *p<0.05 *vs*. WT, $^{\#}$p<0.05 *vs*. respective baseline.

Supplemental Material

Phosphodiesterase 2 Protects against Catecholamine-induced Arrhythmia and Preserves Contractile Function after Myocardial Infarction

Running title: *Vettel et al., PDE2 in arrhythmia and contractile function*

Christiane Vettel, PhD*; Marta Lindner*; Matthias Dewenter, MD*; Kristina Lorenz, PhD; Constanze Schanbacher; Merle Riedel, MD; Simon Lämmle, PhD; Simone Meinecke, MD; Fleur Mason, PhD; Samuel Sossalla, MD; Andreas Geerts; Michael Hoffmann; Frank Wunder, PhD; Fabian J. Brunner, MD; Thomas Wieland, PhD; Hind Mehel, PhD; Sarah Karam, PhD; Patrick Lechêne, BSc; Jérôme Leroy, PhD; Grégoire Vandecasteele, PhD; Michael Wagner, MD; Rodolphe Fischmeister, PhD[†,#]; Ali El-Armouche, MD[†,#]

From the Institute of Experimental and Clinical Pharmacology and Toxicology, University Medical Center Mannheim, Heidelberg University, Germany (C.V., T.W.); Department of Pharmacology, University Medical Center Göttingen (UMG) Heart Center, Georg August University Medical School Göttingen, Germany (C.V., M.D., M.R., S.M.); UMR-S 1180, INSERM, Université Paris-Sud, Université Paris-Saclay, Châtenay-Malabry, France (M.L., H.M., S.K., P.L., J.L., G.V., R.F.); Department of Molecular Cardiology and Epigenetics, University Hospital Heidelberg, Germany (M.D.); Institute of Pharmacology and Toxicology, University of Würzburg and Leibniz-Institut für Analytische Wissenschaften – ISAS – e.V., Dortmund, Germany (K.L., C.S.), Comprehensive Heart Failure Center, University of Würzburg, and West German Heart and Vascular Center Essen, Germany (K.L.); Institute of Pharmacology, University of Technology Dresden, Germany (S.L., M. W., A.EA.); Department of Cardiology and Pneumology, Center of Molecular Cardiology, UMG Heart Center, Georg August University Medical School Göttingen, Germany (F.M., S.S.); Department of Internal Medicine III: Cardiology and Angiology, University of Kiel, Germany (S.S.); BAYER Pharma AG, Wuppertal, Germany (A.G., M.H., F.W.); University Heart Center, Department of General and Interventional Cardiology, University Medical Center Hamburg-Eppendorf (F.J.B.). DZHK (German Centre for Cardiovascular Research), partner sites Heidelberg/Mannheim, Göttingen and Hamburg/Kiel/Lübeck, Germany (C.V., M.D., M.R., S.M., F.M., S.S., F.J.B., T.W.)

[#]Correspondence to Ali El-Armouche, Institute of Pharmacology, University of Technology Dresden, Medical Faculty Carl Gustav August, Fetscherstr. 74, 01307 Dresden, Germany. Phone: +49 351 458 6300, Fax: +49 351 458 6315; e-mail: ali.el-armouche@tu-dresden.de OR Rodolphe Fischmeister, INSERM UMR-S 1180, Université Paris-Sud, Faculté de Pharmacie, 5, Rue J.-B. Clément, F-92296 Châtenay-Malabry Cedex, France. Phone: 33.1.46.83.57.57; Fax 33.1.46.83.54.75; e-mail: rodolphe.fischmeister@inserm.fr

Detailed Methods

All experiments were carried out according to the European Community guiding principles in the care and use of animals (2010/63/UE, 22 september 2010), the local Ethics Committee (CREEA Ile-de-France Sud) guidelines and the French decree n° 2013-118, 1st February 2013 on the protection of animals used for scientific purposes (JORF n°0032, 7 February 2013 p2199, text n° 24). Authorizations were obtained from the Niedersächsisches Landesamt für Verbraucherschutz und Lebensmittelsicherheit (Germany) and Ministère Français de l'Agriculture, de l'Agroalimentaire et de la Forêt (agreement N°B 92-019-01).

Application of BAY 60-7550 for cardiovascular analysis, canine animal model
Evaluation of hemodynamic parameters was performed in beagle dogs according to GLP requirements using a dog model described earlier[1]. Both male and female animals were used at an age of 1 to 5.5 years and 9.5 to 16 kg body weight. Briefly, 12 Beagle dogs were subjected to general neuroleptic anesthesia (droperidol + fentanyl) and mechanical ventilation with nitrous oxide/oxygen (1:3). Administration formulations of BAY 60-7550 (BAY) were prepared in ethanol/polyethylene glycol 400 (1:9 v/v) and administered intraduodenally (i.d.) with an administration volume of 1-2 ml/kg in a dose range of 3, 10, and 30 mg/kg (n=3 dogs per group). Three control animals received the vehicle only. Dogs were instrumented with a Millar tip catheter placed into the abdominal aorta for measurement of systemic arterial blood pressure. A second Millar catheter equipped with a pressure and a velocity sensor was introduced into the heart via the left carotid artery. The pressure sensor was located within the left ventricle, the velocity sensor located in the ascending aorta to allow the measurement of stroke volume, left ventricular pressure (LVP) and the determination of left ventricular pressure rise (LV dP/dt), a surrogate for heart contractility. Heart rate was determined by ECG. Cardiac output (CO) and total peripheral resistance were calculated from stroke volume, heart rate and mean arterial blood pressure. At predefined time points at baseline and up to 240 min after administration, cardiovascular parameters were collected, stored and evaluated using P3 Plus Ponemah software (DSI).

Chronic isoproterenol administration
Isoproterenol (ISO, Sigma-Aldrich) was delivered to mice by subcutaneously implanted osmotic minipumps (Alzet, model 2002) that released ISO solved in 0.9% NaCl at a dose of 30 µg/g/d[2]. Anesthesia was performed with isoflurane (1.5% v/v). After 7 days, cardiac function was monitored by echocardiography. The mice used for this study were 2 month old littermates with a FVB/N background. Groups were age and sex matched.

Echocardiography
Animals were kept under light temperature and ECG-controlled anesthesia (isoflurane, 1.5% v/v or pentobarbital 35 mg/kg body weight (i.p.)) during the whole procedure. Echocardiography images (Vevo 770® System or 2100® System (MI), Visual Sonics Inc.) were obtained in a parasternal long and a short axis view at midpapillary and apical (representative M-mode pictures, MI) muscle level at a frame rate of 60 Hz. Long axis images were used to measure left ventricle length (L) during end-diastole (d) and end-systole (s). The thickness of the anterior (AWTh) and posterior wall (PWTh), the left ventricular diameter (LVD), the epicardial (EpiA) and endocardial (EndoA) area of the left ventricular cavity were obtained in the short axis or long axis (MI) view during d and s stages. Parameters were calculated as follows: %Fractional area shortening (%FAS) = (EndoAd – EndAs)/EndAd x 100; systolic volume (SV) = 5/6 x (EndoAd x Ld – EndoAs x Ls); cardiac output CO=SV x HR/1000; left ventricular weight (LVW) = 1.05 x 5/6 x [EpiAs x (Ls + (AWThs + PWThs)/2)) – EndoAs x Ls], where 1.05 is the specific gravity of muscle. %Ejection fraction = 100* ((7.0 / (2.4 + average diastolic diameter)* (average diastolic diameter)^3) – (7.0 / (2.4 + average systolic diameter) * (average systolic diameter)^3) / ((7.0 / (2.4 + average diastolic diameter)* (average diastolic diameter)^3). In MI, measurements were performed before and two weeks after left anterior descending coronary artery ligation.

Longevity study
Animals were kept under standard housing conditions until either natural death or any severe illness occurred (e.g. tumor growth, colic, age related decay etc.). Animals, which fell sick during the study were euthanized according to animal care guidelines to avoid unnecessary pain and counted as a naturally death event. The study was terminated after 38 months with 3 still living individuals. Groups were age and sex matched.

Implantation of ECG transmitters
Mice were anaesthetized with isoflurane (2% v/v) via mask ventilation and placed on a warming plate (37°). After the skin of the anterior thoracic region was depilated and disinfected, a 2 cm long median incision of the thoracic skin was made. The underlying tissue was prepared in order to create subcutaneous space for the ECG-transmitter (Data Sciences International, ETA-F10) and the electrodes. Afterwards, the ECG-transmitter was placed subcutaneously to the back of the mouse, the negative electrode was fixed to the right pectoralis fascia and the positive electrode was fixed 1 cm left to the xiphoid. The wound was closed using resorbable sutures. Alternatively, the transmitters were implanted into the peritoneal cavity. Buprenorphine 0.05 mg/kg s.c. once before starting the surgical procedure and metamizol 300 mg/kg p.o. from 2 days before to 7 days after the surgical procedure were used for intra- and postoperative analgesia. Recordings were started after a recovery time of at least two weeks post subcutaneous implantation of the telemetric transmitter). Recording and analysis parameters were set according to the manufacturer's instructions using P3 Plus software (DSI) or LabChart software (Chart 5.4, AD Instruments) and to conventional arrhythmia/frequency analysis guidelines[3-5]. Heart rate, activity and RR-intervals are given as either an average of 1 min or of 5 s intervals. Details are specified in the respective figure legends.

Isolation of adult mouse cardiomyocytes
Ventricular myocytes were obtained from 10 to 14 week old male mice. Animals were anesthetized by intraperitoneal injection of pentothal (150 mg/kg), and the heart was quickly removed and placed into cold Ca^{2+}-free Tyrode's solution containing (in mmol/L): NaCl 113, KCl 4.7, $MgSO_4$ 4, KH_2PO_4 0.6, NaH_2PO_4 0.6, BDM 10, $NaHCO_3$ 1.6, HEPES 10, Taurine 30, D-glucose 20, adjusted to pH 7.4. The ascending aorta was cannulated and the heart was perfused with oxygenated Ca^{2+}-free Tyrode's solution at 37°C during 4 min. For enzymatic dissociation, the heart was perfused with Ca^{2+}-free Tyrode's solution containing liberase TM research grade (Roche Diagnostics) for 10 min at 37°C. Then the heart was removed and placed into a dish containing Tyrode's solution supplemented with 0.2 mmol/L $CaCl_2$ and 5 mg/ml BSA (Sigma-Aldrich). The ventricles were separated from the atria, cut into small pieces, and triturated with a pipette to disperse the myocytes. Ventricular myocytes were filtered on gauze and allowed to sediment by gravity for 10 min. The supernatant was removed and cells were suspended in Tyrode's solution supplemented with 0.5 mmol/L $CaCl_2$ and 5 mg/ml BSA. The procedure was repeated once and cells were suspended in Tyrode's solution with 1 mmol/L $CaCl_2$. Freshly isolated ventricular myocytes were plated in 35 mm culture dishes coated with laminin (10 µg/ml) and stored at room temperature until use[6].

cAMP measurements by FRET
Adult mouse ventricular myocytes isolated from WT or PDE2-TG mice were infected with an adenovirus encoding the Epac-S^{H187} cAMP FRET probe for 24 h (kindly provided by Dr. Kees Jalink, Cancer Institute, Amsterdam, The Netherlands)[7]. Thereafter, the cells were washed once and maintained in a physiological buffer containing (in mmol/L): NaCl 144, KCl 5.4, $CaCl_2$ 1.8, $MgCl_2$ 1.8, and HEPES 20, pH 7.4 at room temperature. Images were captured every 5 s using the ×40 oil immersion objective of an inverted microscope (Nikon) connected to a Cool SNAP HQ2 camera (Photometrics) controlled by the Metafluor software (Molecular Devices). Cyan Fluorescent Protein (CFP) was excited for 300 ms by a Xenon lamp (Nikon) using a 440/20BP filter and a 455LP dichroic mirror. Dual-emission imaging of CFP and Yellow Fluorescent Protein (YFP) was performed using a Dual-View emission splitter

equipped with a 510 LP dichroic mirror and BP filters 480/30 and 535/25 nm, respectively. The YFP/CFP emission ratio upon 436 nm excitation (filters YFP 535 ± 15 nm, CFP 480 ± 20 nm) was measured. After each measurement, emission values were corrected for bleedthrough of CFP into the YFP channel. The imaging data was analyzed with Excel. All experiments were performed at room temperature.

$I_{Ca,L}$ measurements

The whole-cell configuration of the patch-clamp technique was used to record $I_{Ca,L}$. Pipette resistance was between 1–2 MΩ when filled with internal solution containing (in mmol/L): CsCl 118, EGTA 5, $MgCl_2$ 4, sodium phosphocreatine 5, Na_2ATP 3.1, Na_2GTP 0.42, $CaCl_2$ 0.062 (pCa 8.5), HEPES 10, adjusted to pH 7.3 with CsOH. Extracellular Cs^+-Ringer solution contained (in mmol/L): $CaCl_2$ 1.8, $MgCl_2$ 1.8, NaCl 107.1, CsCl 20, $NaHCO_3$ 4, NaH_2PO_4 0.8, D-glucose 5, sodium pyruvate 5, HEPES 10, adjusted to pH 7.4 with NaOH. For $I_{Ca,L}$ measurement, the cells were depolarized every 8 s from -50 to 0 mV for 400 ms and the maximal amplitude of whole-cell $I_{Ca,L}$ was measured as previously described[8]. The use of -50 mV as holding potential allowed the inactivation of voltage dependent sodium currents. K^+ currents were blocked by replacing all K^+ ions with external and internal Cs^+. Currents were not compensated for capacitance and leak currents. All experiments were performed at room temperature.

Measurements of Ca^{2+} transients, sarcomere shortening, SR Ca^{2+} leak and load

All experiments were performed at room temperature within 6 h after cell isolation. Isolated mouse ventricular cardiomyocytes were loaded with 3 µmol/L Fura-2 AM (Invitrogen) for 15 min in Ringer's solution containing (in mmol/L): KCl 5.4; NaCl 121.6; Na-pyruvate 5; $NaHCO_3$ 4.013; NaH_2PO_4 0.8; $CaCl_2$ 1.0; $MgCl_2$ 1.8; glucose 5 and HEPES 10 (pH 7,4 with NaOH). Sarcomere shortening and Fura-2 ratio (measured at 512 nm upon excitation at 340 and 380 nm) were simultaneously recorded in Ringer's solution, using a double excitation spectrofluorimeter coupled with a video detection system (IonOptix, Milton, MA, USA). Myocytes were electrically stimulated with biphasic field pulses (5 V, 4 ms) at a frequency of 0.5 Hz as previously described[9]. Because arrhythmias depend on the initial quality of cells, cardiomyocytes exhibiting spontaneous Ca^{2+} waves (sCaW) when perfused with control Ringer solution were discarded.

SR Ca^{2+} leak and load were measured according to a dedicated protocol[10]. Fura-2 loaded ventricular myocytes were paced by field stimulation at 0.5 Hz in normal Ringer's for few minutes until cellular Ca^{2+} transients reached a steady state. Directly after the last pulse, normal Ringer's was substituted for 30 s by a $0Na^+/0Ca^{2+}$ Ringer's in which Na^+ was replaced by Li^+ and supplemented with 10 mmol/L EGTA. This condition allowed measuring intracellular Ca^{2+} levels in a closed system without trans-sarcolemmal Ca^{2+} fluxes. Then, the cell was switched back to normal Ringer's and paced at 0.5 Hz until Ca^{2+} transient amplitude and sarcomere shortening reached steady-state. Again, following the last pulse, cells were perfused for 30 s with a $0Na^+/0Ca^{2+}$ solution including 1 mmol/L of the RyR2 inhibitor tetracaine. As a consequence, SR Ca^{2+} leak into the cytoplasm was prevented. SR Ca^{2+} leak was estimated as the difference between the Fura-2 ratio recorded at the end of the $0Na^+/0Ca^{2+}$ Ringer's perfusion with and without tetracaine. At the end of this protocol, tetracaine was washed out for at least 60 seconds and 10 mmol/L caffeine was applied to evaluate the total SR Ca^{2+} content.

Ca^{2+} transient amplitude was measured by dividing the twitch amplitude (difference between the end-diastolic and the peak systolic ratios) by the end-diastolic ratio, thus corresponding to the percentage of variation in the Fura-2 ratio. Similarly, sarcomere shortening was assessed by its percentage of variation, which is obtained by dividing the twitch amplitude (difference between the end-diastolic and the peak systolic sarcomere length) by the end-diastolic sarcomere length. Relaxation was assessed by measuring the time-to-50% relaxation from the time to peak shortening, and the Ca^{2+} transient decay was evaluated by measuring the time-to-50% decay of the Fura-2 ratio from the time to peak ratio. SR Ca^{2+} leak was measured by subtracting the ratio of fluorescence recorded in steady-state in

$0Na^+/0Ca^{2+}$ Ringer's with tetracaine from the ratio recorded in steady-state in $0Na^+/0Ca^{2+}$ Ringer's without tetracaine. SR Ca^{2+} load was estimated by dividing the amplitude of the caffeine-induced twitch (difference between the peak ratio obtained with caffeine and the diastolic ratio measured before tetracaine treatment) by the diastolic ratio. Fractional release was calculated by dividing the Ca^{2+} transient amplitude by the caffeine-induced twitch amplitude, thus corresponds to the fraction of Ca^{2+} released from the SR during a twitch. All parameters were calculated offline using IonWizard 6 (IonOptix).

Ca^{2+} spark analysis

Mice were sacrificed under isoflurane anesthesia (5% v/v) by cervical dislocation. 100 I.U. heparin was administered by intraperitoneal injection prior to isolation, to ensure sufficient perfusion of myocardium. Explanted hearts were retrogradely perfused on a Langendorff system, first with a Ca^{2+} free solution containing (in mmol/L) NaCl 113, KCl 4.7, KH_2PO_4 0.6, $Na_2HPO_4x2H_2O$ 0.6, $MgSO_4x7H_2O$ 1.2, $NaHCO_3$ 12, $KHCO_3$ 10, HEPES 10, taurine 30, BDM 10, glucose 5.5, phenol-red 0.032 (37°C, pH 7.4), followed by the addition of 7.5 mg/ml liberase 1 (Roche diagnostics) and trypsin 0.6% (Life Technologies) as well as 0.125 mmol/L $CaCl_2$. Upon becoming flaccid, ventricular and atrial myocardium were separated. Ventricular myocardium was cut into small pieces and dispersed in solution. Ca^{2+} concentration was increased in steps every 7 min until desired concentration was reached. Cells were plated on laminin-coated recording chambers and left to settle for 20 min.

Isolated mouse ventricular cardiac myocytes were incubated for 15 min at room temperature with a Fluo-3 AM loading buffer (10 µmol/L, Molecular Probes). Experimental solution contained (in mmol/L): KCl 4, NaCl 140, $MgCl_2$ 1, HEPES 5, glucose 10, $CaCl_2$ 2 (pH 7.4, NaOH, room temperature) plus isoproterenol (ISO) 100 nmol/L for the ISO experiments. Myocytes were superfused with experimental solution for 5-10 min before experiments commenced and during experiments to remove excess indicator and to allow time for complete deesterification of Fluo-3 AM. Ca^{2+} spark measurements were carried out on a laser scanning confocal microscope (LSM 5 Pascal, Zeiss) with a 40x oil-immersion objective. Fluo-3 was excited by an argon ion laser (488 nm). Emitted fluorescence was collected through a 505 nm long-pass emission filter. Fluorescence images were recorded in the line-scan mode (width of scan line: 38.4 µm, 512 pixels per line, pixel time: 0.64 µs, number of unidirectional line scans: 10,000, measurement period: 7.68 s). Confocal line scans were performed at rest after a brief period of field stimulation to load the SR (10 pulses, 1 Hz, 20 V). Ca^{2+} sparks were analyzed in SparkMaster for ImageJ. Mean spark frequency (CaSpF) was normalized to cell width and scan rate (100 $\mu m^{-1}*s^{-1}$).

Immunoblot analysis

Protein samples were prepared from pulverized ventricular myocardium and lyzed in buffer containing 30 mmol/L Tris/HCl (pH 8.8), 5 mmol/L EDTA, 30 mmol/L NaF, 3% SDS, and 10% glycerol. Samples were separated in denaturizing acrylamide gels and subsequently transferred onto nitrocellulose or PVDF membranes. After blocking the membranes with Roti®-block (Carl Roth) for 1 h, the incubation with anti-PDE2 (1:1,000, FabGennix), anti-calsequestrin (1:1,000, ThermoScientific), and anti-α-tubulin (1:2,000, Sigma-Aldrich) was carried out over night at 4°C. After incubation with appropriate secondary antibodies for 1 h, proteins were visualized by enhanced chemoluminescence and quantified with Quantity One software (Biorad).

Measurement of infarct size

Hearts were fixed in 4% (m/V) paraformaldehyde and embedded in paraffin. Hearts were sliced transversely (2 µm). Sections of the midpapillary region were stained with Sirius Red as described previously[11, 12]. For the determination of the infarct size, the epicardial and endocardial infarct length and circumference was measured. Infarct size was calculated as follows: [(epicardial infarct length/ epicardial circumference) + (endocardial infarct length/endocardial circumference)/2] * 100 [13].

Online Figures

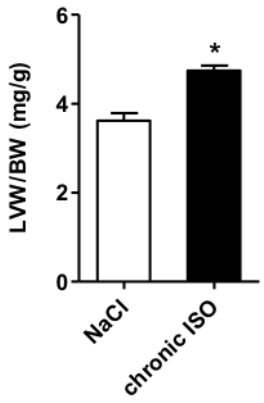

Online Figure I. ISO infusion induces left ventricular hypertrophy. Relative left ventricular weight (LVW) determined by echocardiography to body weight (BW) ratio in mice subjected to chronic ISO infusions (30 mg/kg/d for 7d) or NaCl (0.9%) as control; n=7-9. Statistical significance was determined by Student's *t*-test. *p<0.05 *vs*. NaCl.

A

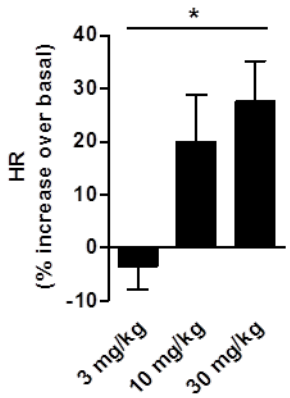

B

	HR beats/min	BPs mmHg	BPd mmHg	LVP mmHg	LV dP/dt mmHg/s	CO l/min	SV ml/beat
basal	78 ± 7.3	123 ± 7.6	71 ± 10.2	105 ± 6.9	2655 ± 133	1.1 ± 0.1	14 ± 2.8
control	74 ± 10.7	118 ± 4.8	68 ± 7.2	102 ± 4.0	2542 ± 68	0.9 ± 0.1	13 ± 2.4
basal	78 ± 3.5	124 ± 5.1	75 ± 5.5	105 ± 4.8	2715 ± 294	0.9 ± 0.1	11 ± 1.3
3 mg/kg	75 ± 2.5	132 ± 7.5	81 ± 6.4	111 ± 6.6	2598 ± 303	0.9 ± 0.1	12 ± 0.9
basal	83 ± 5.3	133 ± 6.7	82 ± 4.0	116 ± 6.4	3562 ± 355	1.1 ± 0.1	13 ± 1.7
10 mg/kg	100 ± 11.6	136 ± 4.6	89 ± 3.5	121 ± 4.9	3489 ± 253	1.2 ± 0.1	12 ± 2.1
basal	78 ± 1.7	126 ± 11.5	79 ± 7.9	110 ± 11.2	3099 ± 477	1 ± 0.2	13 ± 2.4
30 mg/kg	100 ± 7.8	119 ± 10.1	78 ± 6.7	106 ± 9.6	2957 ± 532	1.2 ± 0.4	12 ± 3.4

Online Figure II. Effect of PDE2-specific inhibitor BAY 60-7550 on hemodynamic parameters in beagle dogs. Effect of PDE2 inhibition in dogs exposed to the indicated doses of BAY 60-7550 (i.d.). Animals were anaesthetized, equipped with catheters (abdominal aorta, left ventricle and ascending aorta) and monitored by echocardiography over a period of 240 min post application. (A) Maximal increase in heart rate (HR) given as % over respective basal HR. (B) Table with assessed hemodynamic parameters at the time point of maximal increase in heart rate (HR): systolic and diastolic blood pressure (BPs, BPd), left ventricular pressure (LVP), cardiac output (CO), stroke volume (SV). Average of n=3 for each group. Statistical significance was determined by one-way ANOVA. *p<0.05 for linear trend.

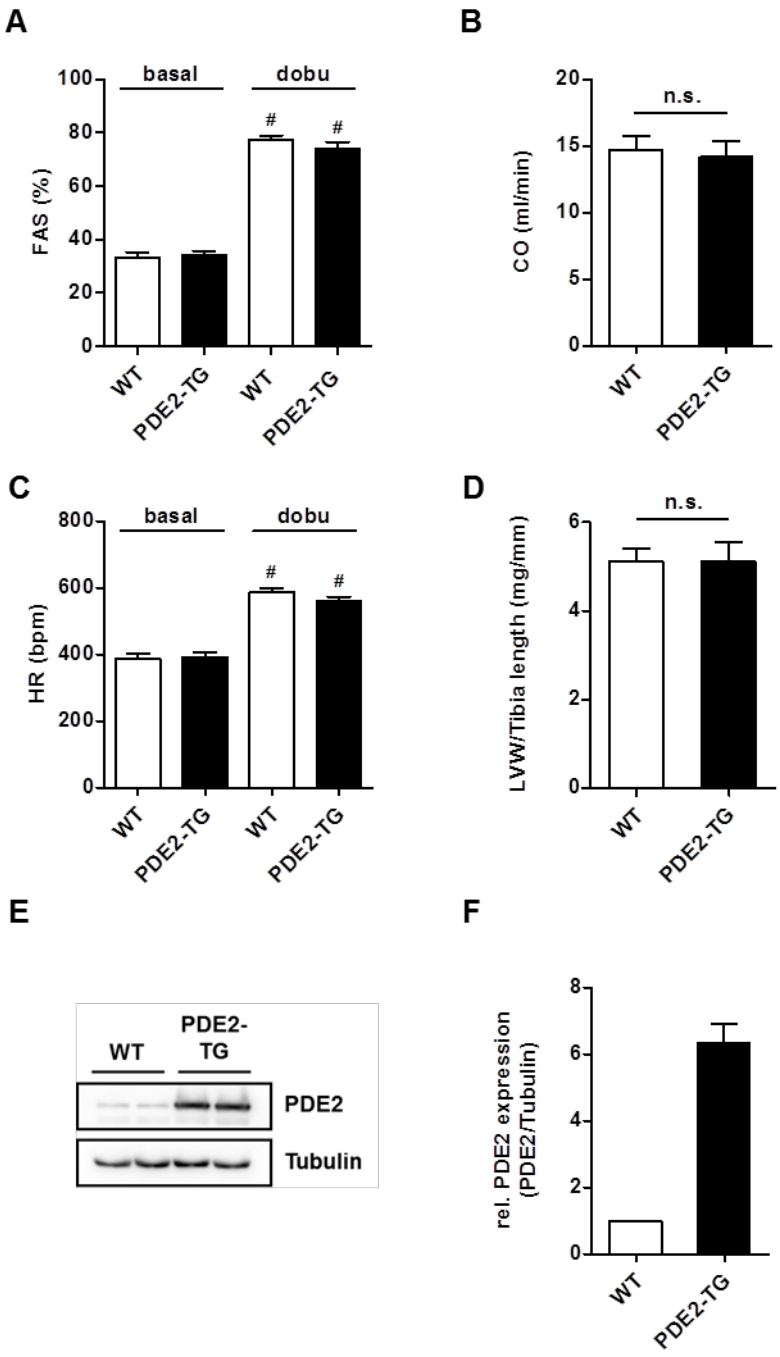

<u>Online Figure III.</u> Characterization of the lower expressing transgenic mouse line TG-4808. Echocardiographic determination of fractional area shortening (FAS, A), cardiac output (CO, B), and heart rate (HR, C) in anaesthetized 2 month old mice. Animals were treated with 10 mg/kg dobutamine (DOBU, i.p.) 2 min prior to measurements when indicated. (D) Left ventricular weight (LVW) calculated from the echocardiographic data and normalized to tibia length; n=12-14 for each group. (E, F) Lysates prepared from ventricular myocardium were analyzed by immunoblot with the indicated specific antibodies. PDE2 expression was normalized to tubulin and given relative to WT. (E) Immunoblots and (F) quantification; n=2 for each group Statistical significance was determined by one-way ANOVA followed by Newman-Keuls multiple comparison Test (A, C) and by Student's *t*-test (B, D). $^{\#}p<0.05$ *vs.* respective basal.

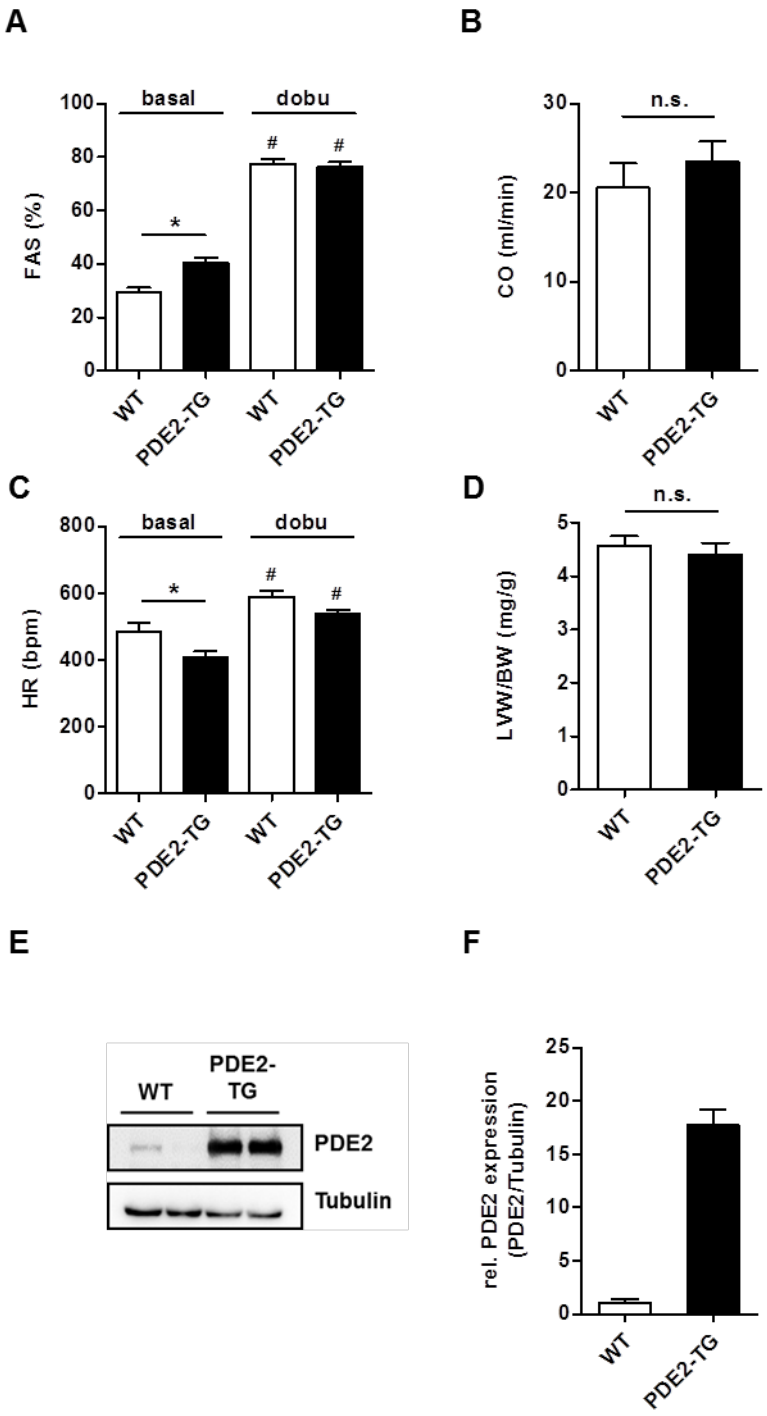

Online Figure IV. Characterization of the high expresser transgenic mouse line TG-4811. Echocardiographic determination of fractional area shortening (FAS, A), cardiac output (CO, B), and heart rate (HR, C) in anaesthetized 2 month old mice. Animals were additionally treated with 10 mg/kg dobutamine (DOBU, i.p.) 2 min prior to measurements when indicated. (D) Left ventricular weight (LVW) calculated from the echocardiographic data and normalized to body weight (BW); n=6-8 for each group. (E, F) Lysates prepared from ventricular myocardium were analyzed by immunoblot with the indicated specific antibodies. PDE2 expression was normalized to tubulin and given relative to WT. (E) Immunoblots and (F) quantification; n=2 for each group. Statistical significance was determined by one-way ANOVA followed by Newman-Keuls multiple comparison test (A, C) and by Student's *t*-test (B, D). *p<0.05 *vs.* WT, $^{\#}$p<0.05 *vs.* respective basal.

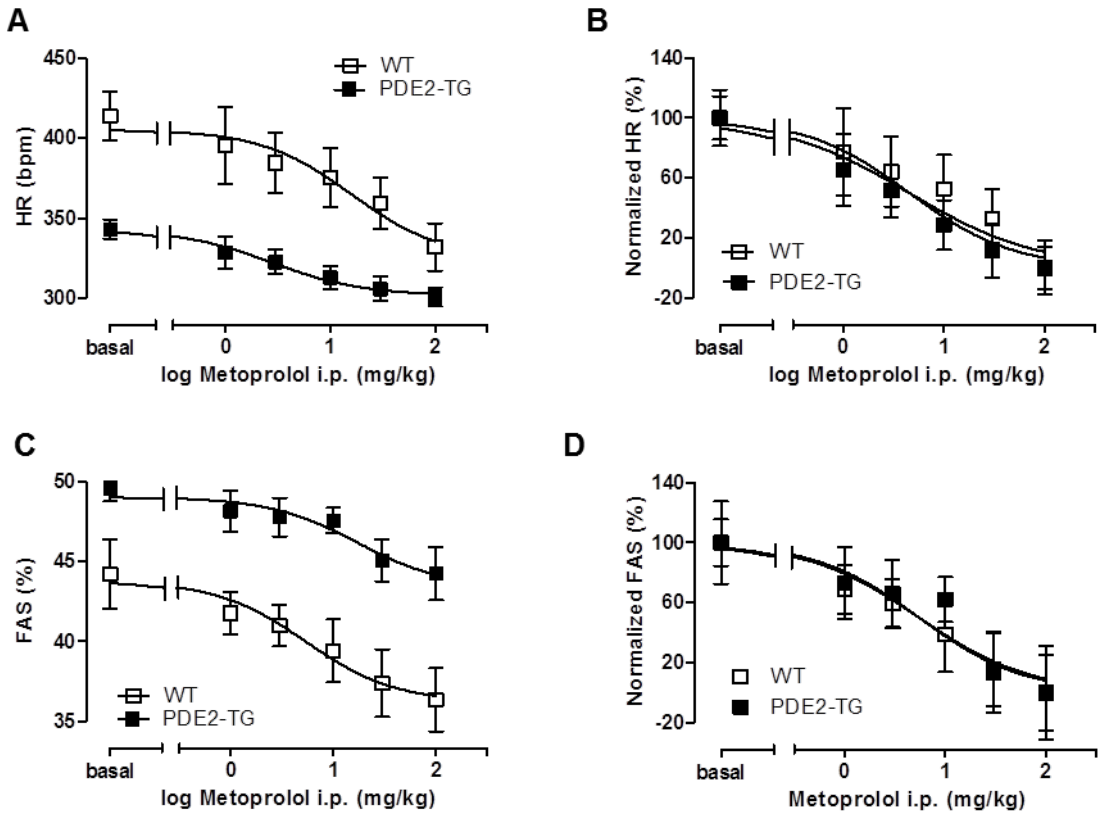

<u>Online Figure V.</u> Metoprolol reduced heart rate to a similar extent in WT and PDE2-TG, while basal hypercontractility of PDE2-TG was independent of β-AR activity. Echocardiographic determination of heart rate (HR, A) and fractional area shortening (FAS, C) in anaesthetized mice in the presence of increasing metoprolol doses (1, 3, 10, 30, 100 mg/kg, i.p.). (B, D) Normalization of A and C to compare potency.

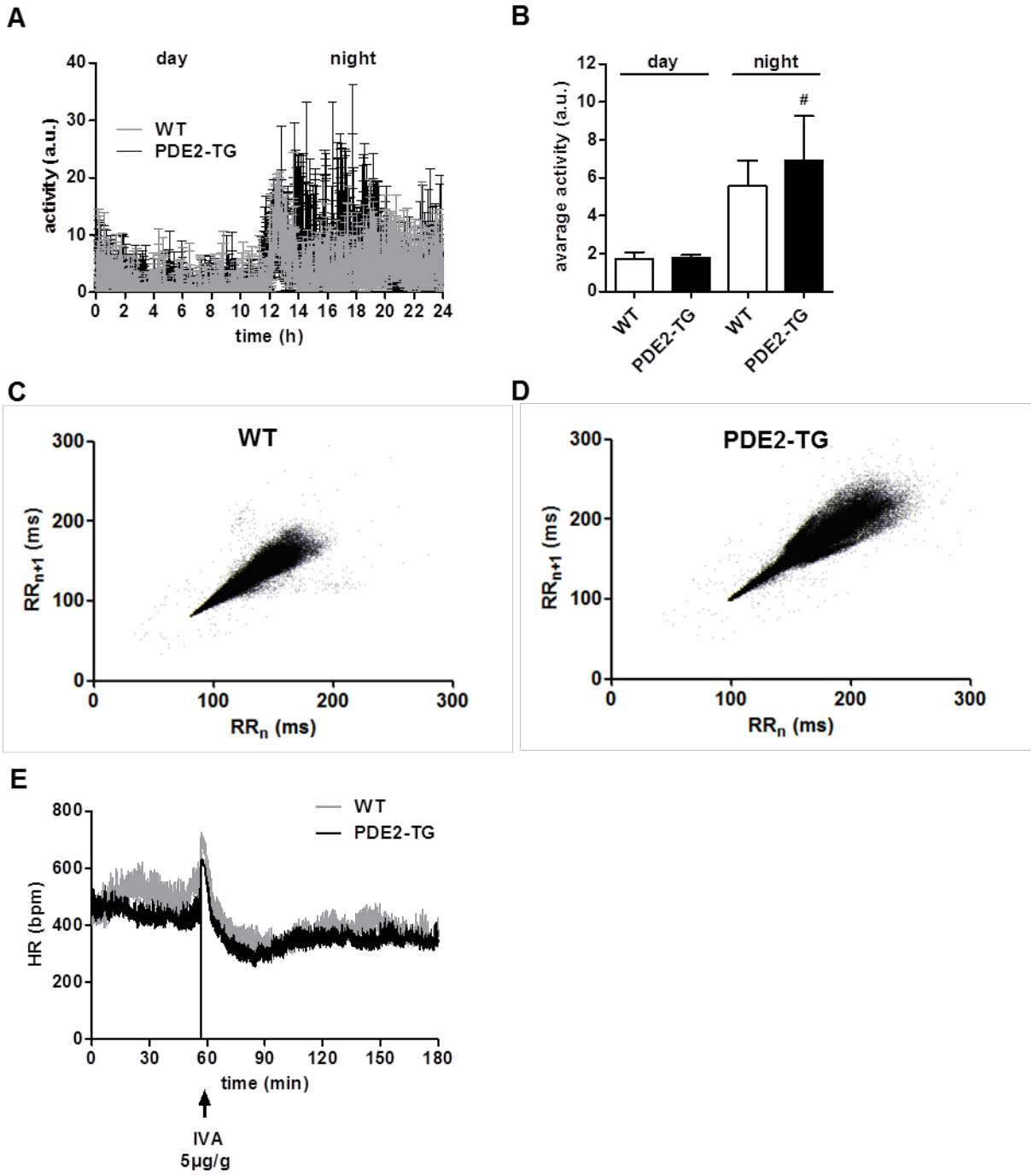

<u>Online Figure VI.</u> ECG-Telemetry: Activity pattern and Poincaré plots of RR intervals documented over a period of 24 h. Application of HCN-Blocker Ivabradine (IVA). Animals (n=4 per genotype) were monitored by ECG-telemetry for a period of 72 h to calculate average changes in activity of a 24 h cycle. Activity was tracked as an avarage of 1 min intervals. (A) Average circadian changes in activity. (B) Average activity during day and night periods. Statistical significance was determined by one-way ANOVA followed by Newman-Keuls multiple comparison test. $^{\#}p<0.05$ *vs.* respective basal. (C, D) Representative Poincaré plot of a WT an TG animal regarding the distribution of daily RR intervals. Sinus arrest and AV block were excluded. (E) Average traces of IVA-application 45 min prior and 2 h after ivabradine (IVA) injection (5 mg/kg, i.p.). Frequencies were tracked as average of 5 s intervals; n=5.

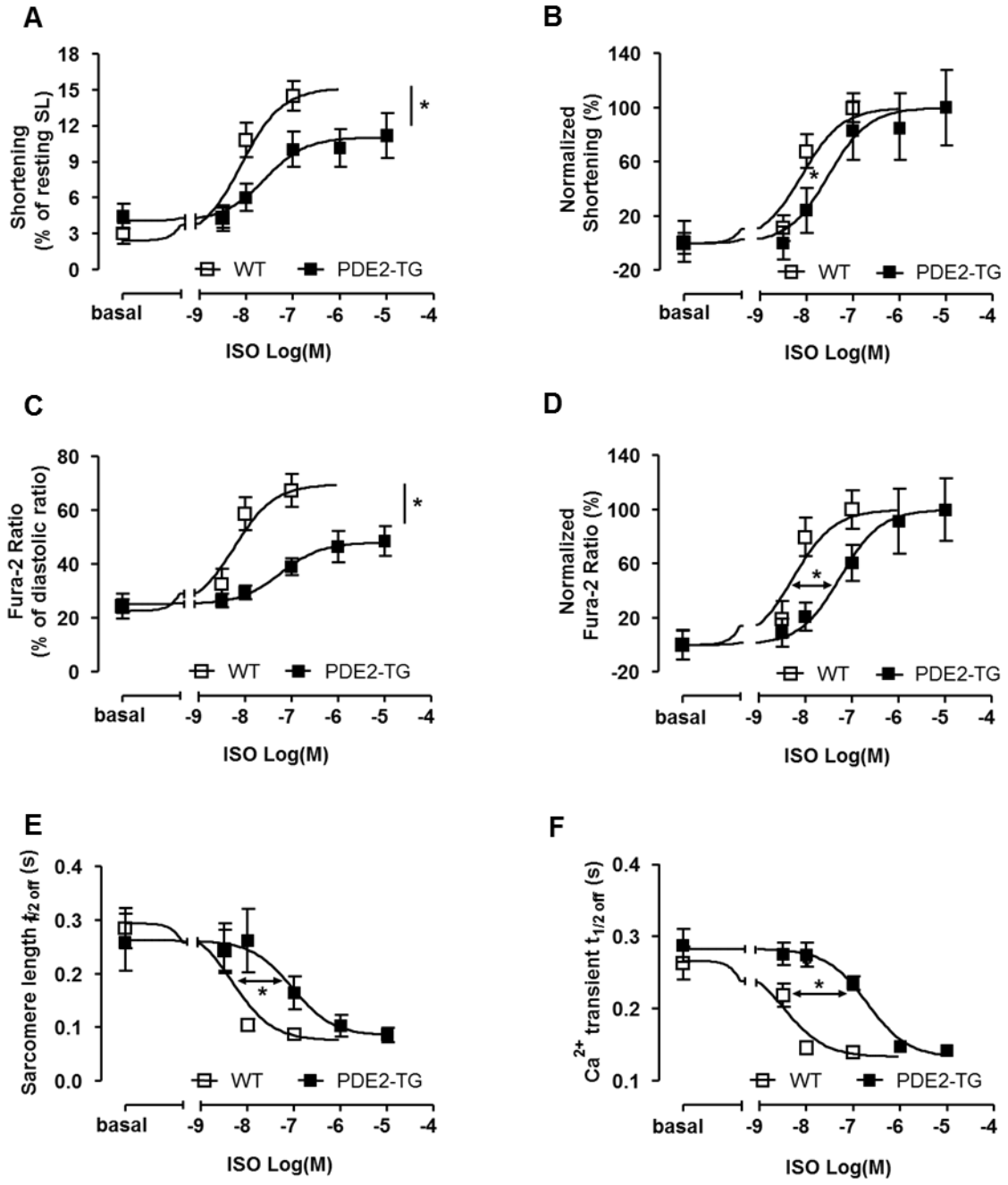

<u>Online Figure VII.</u> PDE2 overexpression attenuates β-AR stimulation of Ca^{2+} transients and sarcomere shortening in cardiomyocytes. Adult ventricular myocytes isolated from WT or PDE2-TG mice were loaded with Fura-2 and stimulated at a frequency of 0.5 Hz in the absence or presence of increasing concentrations of ISO. Sarcomere length and Fura-2 ratio were recorded using an IonOptix System. Concentration-response relationship was extrapolated for WT cardiomyocytes under the assumption that 100 nmol/L ISO is sufficient for maximal responsivness. (A) Average amplitudes of sarcomere shortening. (B) Normalization of (A) to compare $logEC_{50}$ values with lowest values set to 0% and highest values set to 100%. (C) Average amplitudes of Ca^{2+} transients. (D) Normalization of (C) to compare $logEC_{50}$ values with lowest values equal 0% and highest values equal 100%. (E). Average amplitudes of half-time relaxation of sarcomere shortening ($t_{1/2\ off}$). (F) Average

amplitudes of half-time relaxation of Ca^{2+} transients ($t_{1/2\ off}$). n=3-6 animals/genotype with 6-20 cells in each group. Data sets were subjected to comparison of fit (extra sum-of-squares F test) regarding top values (efficacy) or $logEC_{50}$ (potency). *p<0.05 *vs*. WT.

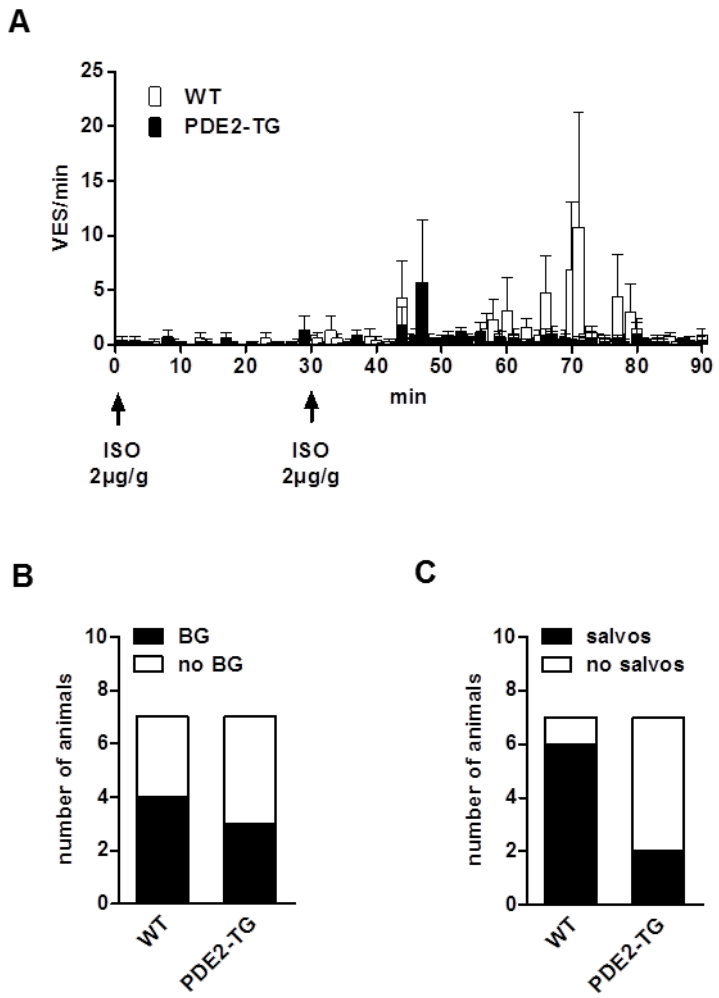

Online Figure VIII. Arrhythmia study in healthy mice. Heart rate was monitored after double ISO injection (2 mg/kg, i.p.; time intervall between injections 30 min) and analyzed for arrhythmic events such as ventricular extra systoles, bigeminy, salvos and VTs over a period of 90 min; n=7. (A) Average ISO-induced ventricular extra systoles (VES including salvos and ventricular tachycardia) per minute. Regular occurence of VES 15 min after the second injection of ISO in all animals. (B) Occurrence of bigemeny (BG) and (C) salvos in addition to main Fig. 4. Statistical significance was determined by Fisher's exact test to compare occurrence of events.

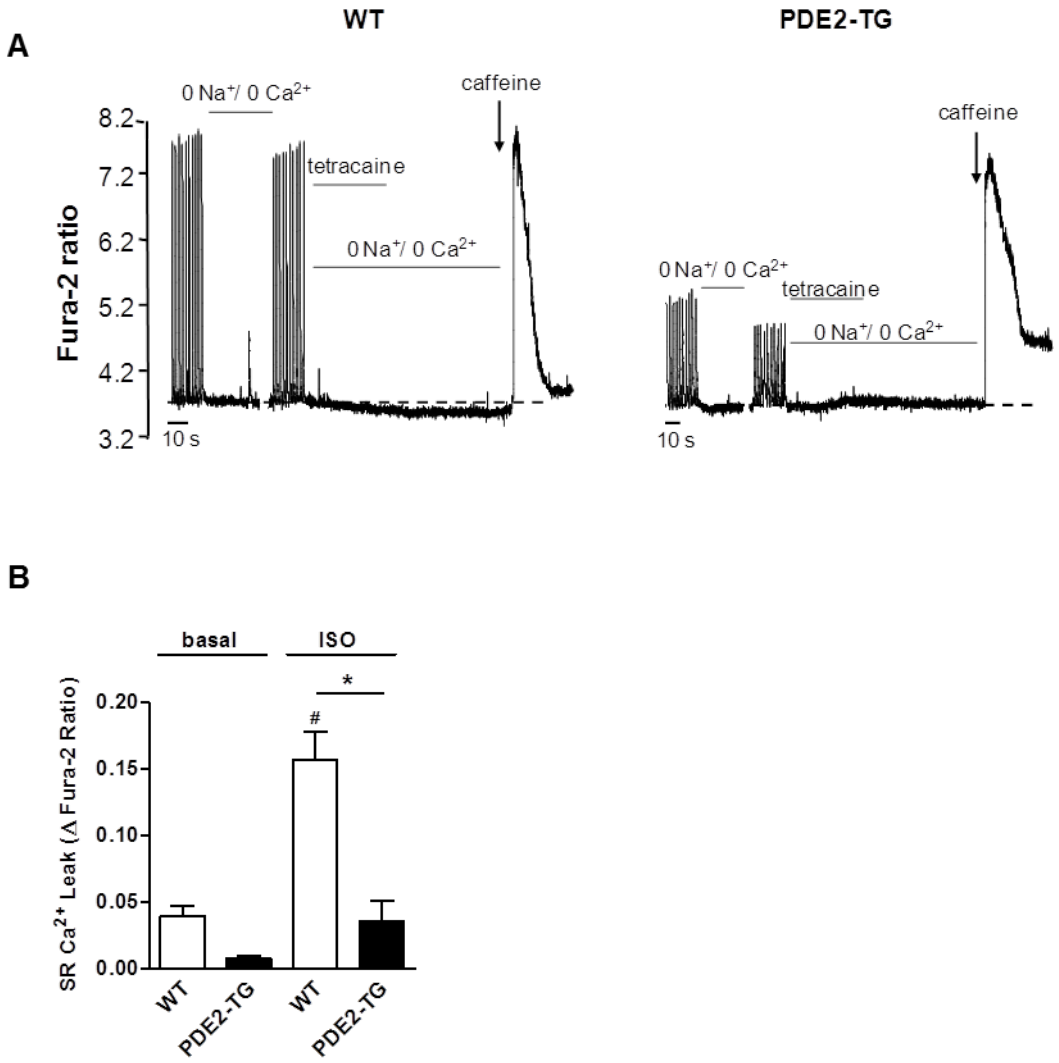

Online Figure IX. SR Ca^{2+} leak (A) Representative traces of Ca^{2+} transients, sarcoplasmic reticulum (SR) Ca^{2+} leak and load measured in Fura-2 loaded adult mouse ventricular myocytes from WT (left) or PDE2-TG mouse (right) paced at 1 Hz, upon ISO (100 nmol/L) application. Tetracaine (1 mmol/L) was used to estimate SR Ca^{2+} leak, caffeine (10 mmol/L) to measure SR Ca^{2+} load. (B) Mean amplitude of the SR Ca^{2+} leak recorded in control or ISO. n=3 animals/genotype with 7-10 cells in each group. Statistical significance was determined by one-way ANOVA followed by Newman-Keuls multiple comparison test. *p<0.05 vs. WT, $^{\#}$p<0.05 *vs*. respective basal.

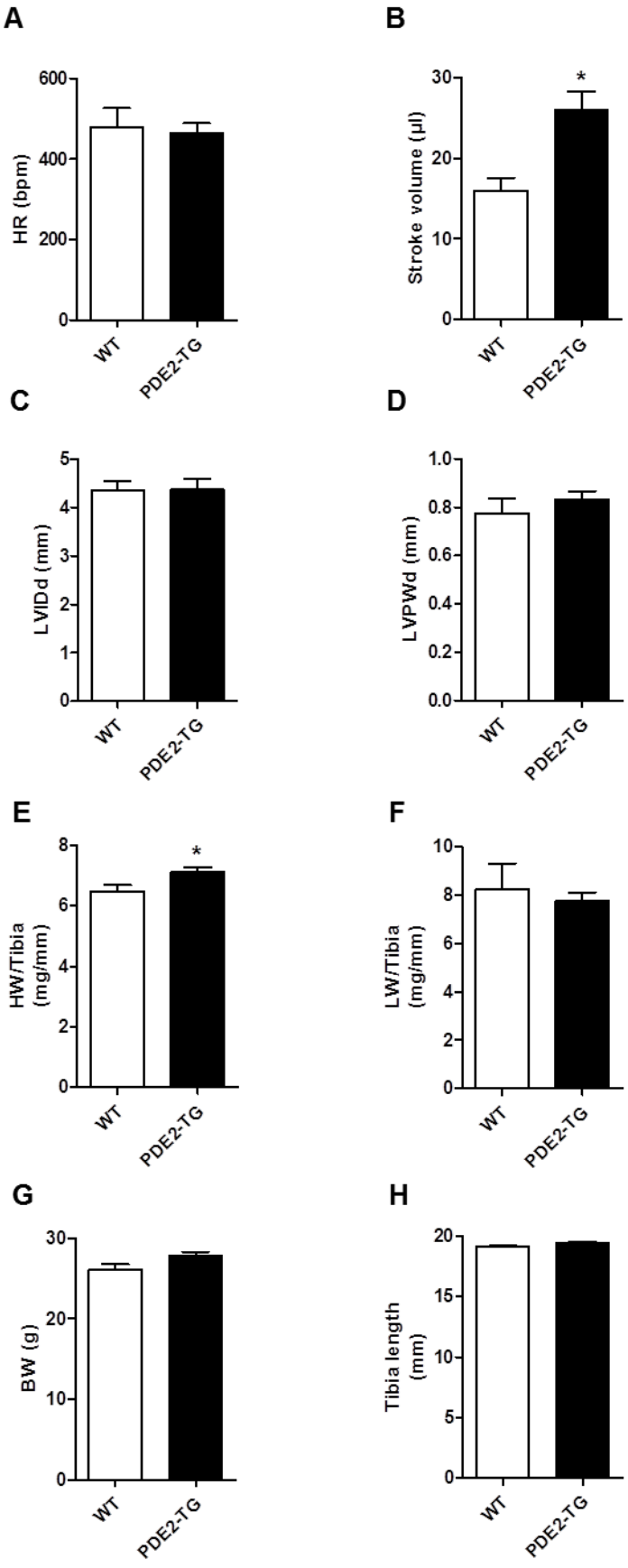

<u>Online Figure X.</u> Echocardiographic parameters and heat weights after MI. Echocardiographic analysis 14 d post MI of (A) heart rate, (B) stroke volume, (C) left

ventricular inner end-diastolic diameter and (D) left ventricular posterior wall end-diastolic diameter**.** Biometric data included determination of (E) heart weight (HW) to tibia length ratios, (F) lung weight (LW) to tibia length ratios, (G) body weight (BW) and (H) tibia length. Statistical significance was determined by Student's *t*-test. *p<0.05 *vs.* WT.

Supplemental References

1. Vormberge T, Hoffmann M, Himmel H. Safety pharmacology assessment of drug-induced qt-prolongation in dogs with reduced repolarization reserve. *Journal of pharmacological and toxicological methods*. 2006;54:130-140
2. El-Armouche A, Wittkopper K, Degenhardt F, Weinberger F, Didie M, Melnychenko I, Grimm M, Peeck M, Zimmermann WH, Unsold B, Hasenfuss G, Dobrev D, Eschenhagen T. Phosphatase inhibitor-1-deficient mice are protected from catecholamine-induced arrhythmias and myocardial hypertrophy. *Cardiovascular research*. 2008;80:396-406
3. Heart rate variability. Standards of measurement, physiological interpretation, and clinical use. Task force of the european society of cardiology and the north american society of pacing and electrophysiology. *European heart journal*. 1996;17:354-381
4. Thireau J, Zhang BL, Poisson D, Babuty D. Heart rate variability in mice: A theoretical and practical guide. *Experimental physiology*. 2008;93:83-94
5. Walker MJ, Curtis MJ, Hearse DJ, Campbell RW, Janse MJ, Yellon DM, Cobbe SM, Coker SJ, Harness JB, Harron DW, et al. The lambeth conventions: Guidelines for the study of arrhythmias in ischaemia infarction, and reperfusion. *Cardiovascular research*. 1988;22:447-455
6. Borner S, Schwede F, Schlipp A, Berisha F, Calebiro D, Lohse MJ, Nikolaev VO. Fret measurements of intracellular camp concentrations and camp analog permeability in intact cells. *Nature protocols*. 2011;6:427-438
7. Klarenbeek J, Goedhart J, van Batenburg A, Groenewald D, Jalink K. Fourth-generation epac-based fret sensors for camp feature exceptional brightness, photostability and dynamic range: Characterization of dedicated sensors for flim, for ratiometry and with high affinity. *PloS one*. 2015;10:e0122513
8. Verde I, Vandecasteele G, Lezoualc'h F, Fischmeister R. Characterization of the cyclic nucleotide phosphodiesterase subtypes involved in the regulation of the l-type ca2+ current in rat ventricular myocytes. *British journal of pharmacology*. 1999;127:65-74
9. Leroy J, Richter W, Mika D, Castro LR, Abi-Gerges A, Xie M, Scheitrum C, Lefebvre F, Schittl J, Mateo P, Westenbroek R, Catterall WA, Charpentier F, Conti M, Fischmeister R, Vandecasteele G. Phosphodiesterase 4b in the cardiac l-type ca(2)(+) channel complex regulates ca(2)(+) current and protects against ventricular arrhythmias in mice. *The Journal of clinical investigation*. 2011;121:2651-2661
10. Shannon TR, Ginsburg KS, Bers DM. Quantitative assessment of the sr ca2+ leak-load relationship. *Circulation research*. 2002;91:594-600
11. Lorenz K, Schmitt JP, Schmitteckert EM, Lohse MJ. A new type of erk1/2 autophosphorylation causes cardiac hypertrophy. *Nature medicine*. 2009;15:75-83
12. Schmid E, Neef S, Berlin C, Tomasovic A, Kahlert K, Nordbeck P, Deiss K, Denzinger S, Herrmann S, Wettwer E, Weidendorfer M, Becker D, Schafer F, Wagner N, Ergun S, Schmitt JP, Katus HA, Weidemann F, Ravens U, Maack C, Hein L, Ertl G, Muller OJ, Maier LS, Lohse MJ, Lorenz K. Cardiac rkip induces a beneficial beta-adrenoceptor-dependent positive inotropy. *Nature medicine*. 2015;21:1298-1306
13. Takagawa J, Zhang Y, Wong ML, Sievers RE, Kapasi NK, Wang Y, Yeghiazarians Y, Lee RJ, Grossman W, Springer ML. Myocardial infarct size measurement in the mouse chronic infarction model: Comparison of area- and length-based approaches. *Journal of applied physiology*. 2007;102:2104-2111